# CHAPTER 4

# RESULT AND DISCUSSION

## 4.1 Introduction

To understand ABL structure in Thailand, which is predominantly under monsoon, lidar data has been chosen to analyze together with radiosonde and surface meteorological data. We selected the data from October 2001 to October 2002 to represent ABL structure because data was almost continuously obtained throughout the year (Figure 3.2).

According to backscattering intensity data, the data was divided into three periods, namely, Period A, B and, C by ABL structure which described as below.

## 4.2 Period A (mid November to late January)

Period A began at mid November 2001 to late January 2002 that is cold season of Thailand. The cloud suddenly disappeared from backscattering intensity data which was observed at mid of November 2001. The ABL consists of high aerosol concentration and top of ABL is almost constant at 2 - 2.5 km especially, from late December to early January (Figure 4.1).

In Period A, radiosonde observation was carried out during 22$^{nd}$ – 24$^{th}$ January 2002. In 22$^{nd}$ and 24$^{th}$ January, radiosonde was launched every 6 hours and in 23$^{rd}$ January every 3 hours (Table 3.2). Therefore the data that collected at 23$^{rd}$ January was selected to represent Period A (Table 1.1).

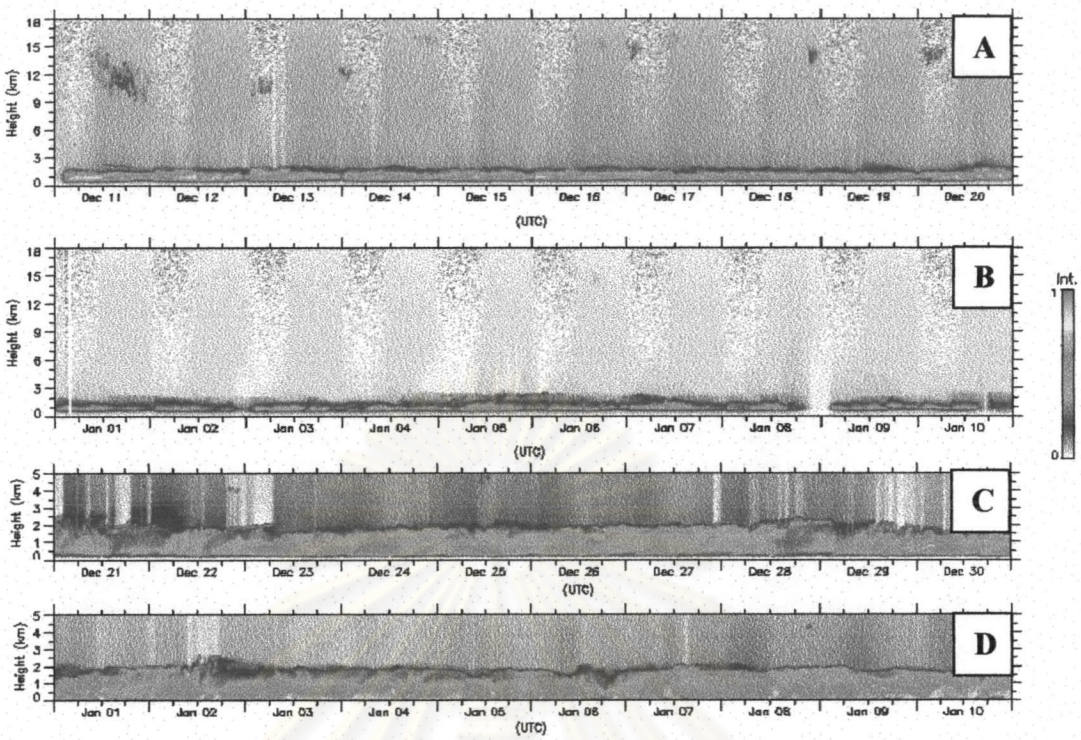


Figure 4.1 Backscattering intensity data show ABL structure in Period A. The data obtained at December 1997 (A) and January 1998 (B) by MPL, and December 2001 (C) and January 2002 (D) by Mie Scattering Lidar

### 4.2.1 Surface Meteorological data

According to TMD annual report year 2001, ridge of high pressure moved from China to cover north of Thailand in October 2001. Amount of rain and temperature decreased from November 2001. This phenomenon became clear in the second week of November 2001. Average pressure and temperature observed at Sukhothai, was about 1013.61 hPa and 23°C, respectively (Figure 4.2).

Average temperature increased all the part of Thailand including the Observatory area in early December 2001.

Ridge of high pressure moved to cover the Observatory area again from late December 2001 to mid of January 2002. Average pressure and temperature was about 1015.66 hPa and 24.16 °C, respectively in this period (Figure 4.2).

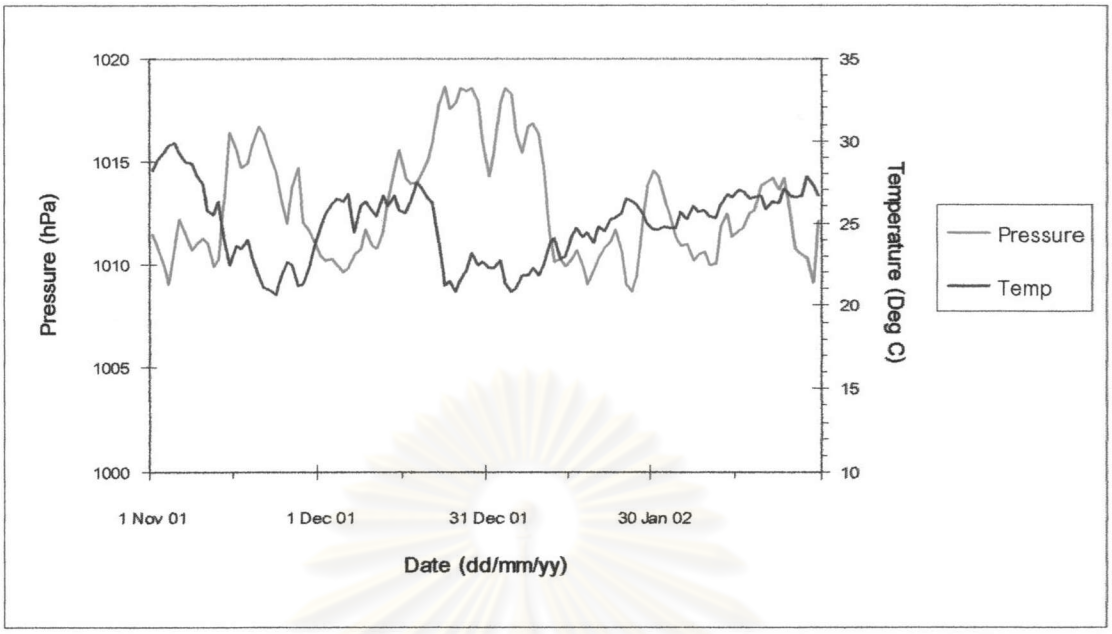


Figure 4.2 Surface pressure and temperature data in Period A

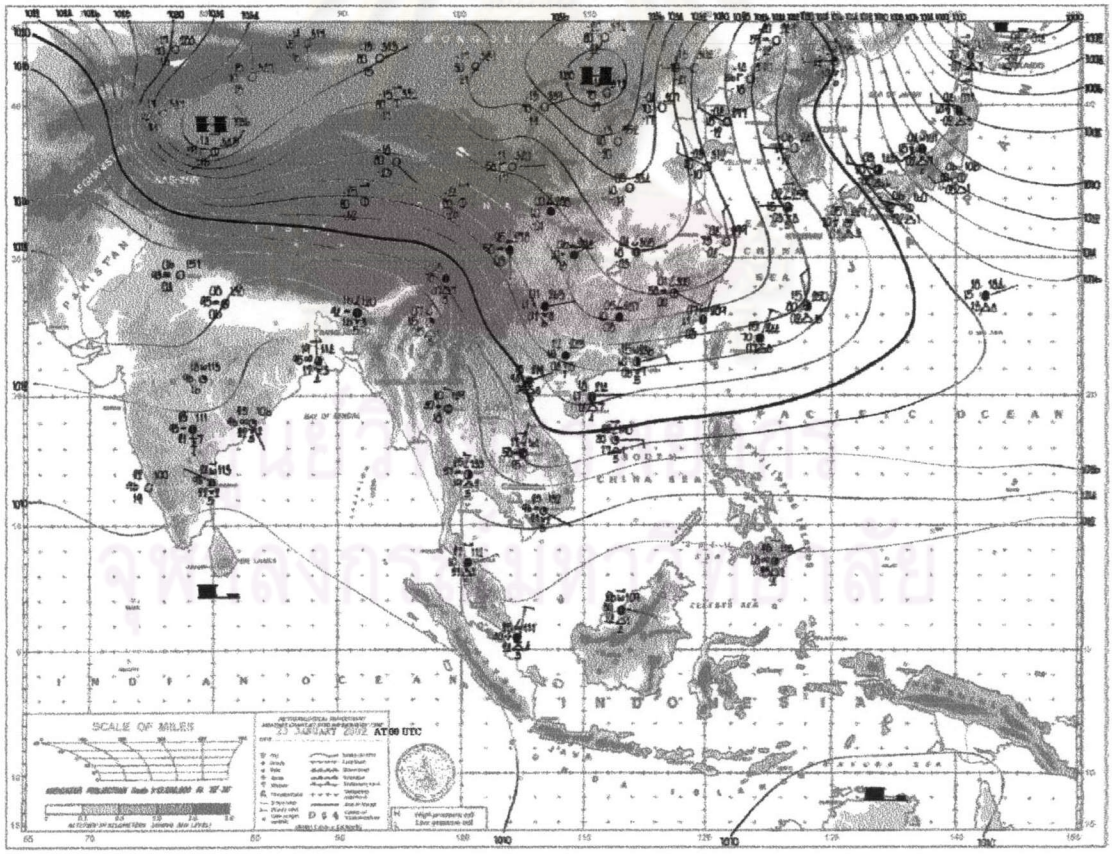


Figure 4.3 Weather map of 23rd January 2002

According to TMD daily report on 23rd January 2001, ridge of high pressure or cool air covered north of Thailand (Figure 4.3).

### 4.2.2 Radiosonde data

Radiosonde data was grouped into three periods according to the influence of solar radiation, namely, period before 09:00 a.m., period from 09:00 a.m. to 03:00 p.m., and period after 03:00 p.m., following Menut (1999). The radiosonde data analysis show as below;

#### 4.2.2.1 Period before 09:00 a.m.

The vertical profile of temperature and potential temperature data shows strong inversion and uniform potential temperature layers at 2.8 and 4 km. This is the large scale feature of cold air advect into the area inversion aloft. Resulting is the stratified layer to convect up. Top of ABL is not clear in vertical profile of potential temperature and temperature data because top of ABL is always mixed with bottom of strong convection above to form stable layer from 2 to 3 km. Stable boundary layer formed at 200 m due to surface inversion at 06:00 a.m. (Figure 4.4 and 4.5).

For vertical profile of wind data, variation in wind speed occurred from surface up to 2 km before increasing as hyperbola (Figure 4.6). Wind direction changed from north to east from 2 km up indicates colder air mass advection to this region (Figure 4.7).

According to vertical profile of relative humidity, there are two high humidity layers at 2 km and 4 km. Top of ABL can identify by top of lower high humidity layer that is block humidity diffusion to above. It corresponds to vertical profile of wind data that is dry and cold air advection to this area (Figure 4.8).

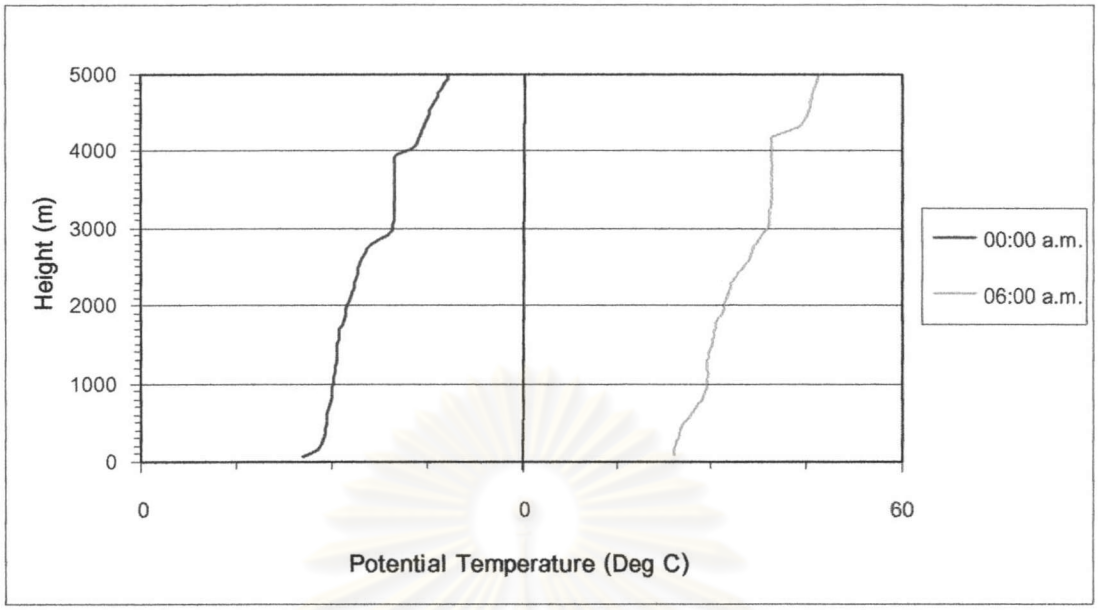


Figure 4.4 Vertical profile of potential temperature observed during 00:00 a.m. – 06:00 a.m., 23rd January 2002.

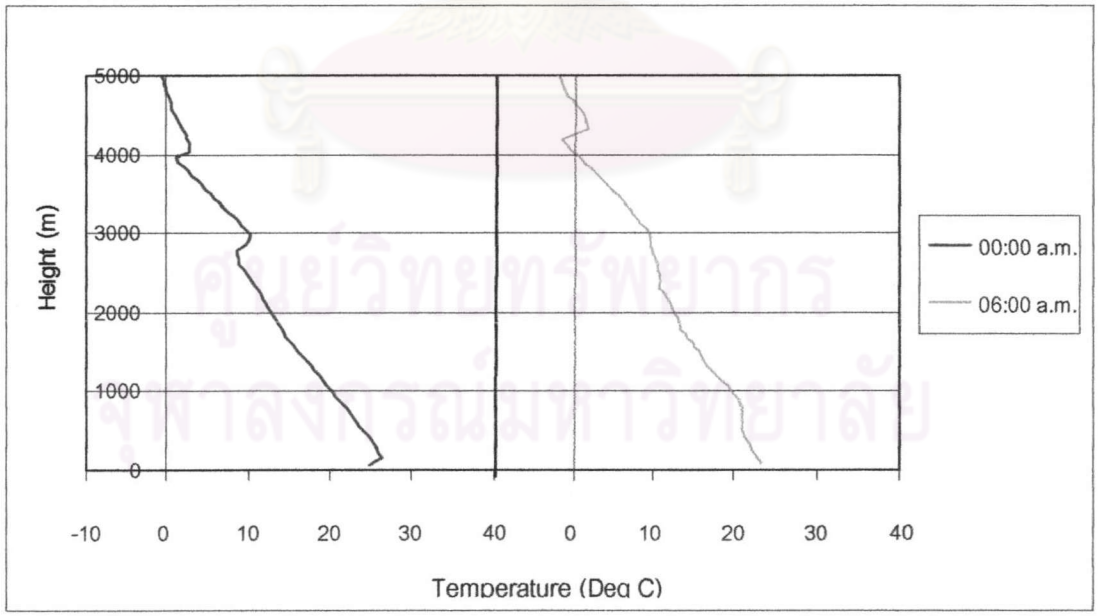


Figure 4.5 Vertical profile of temperature observed during 00:00 a.m. – 06:00 a.m., 23rd January 2002.

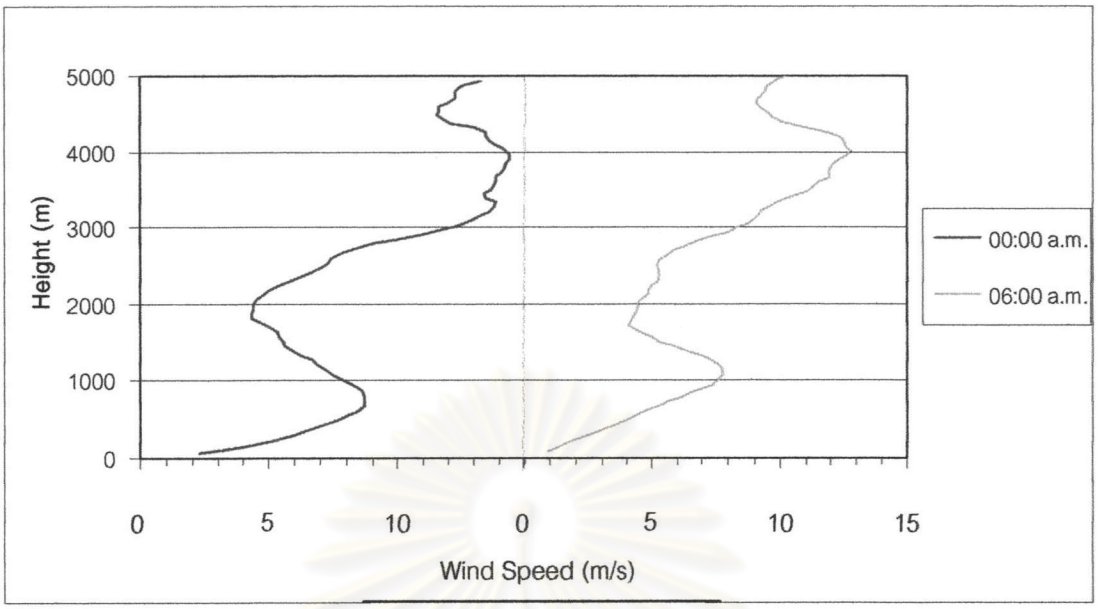


Figure 4.6 Vertical profile of Wind Speed observed during 00:00 a.m. – 06:00 a.m., 23rd January 2002.

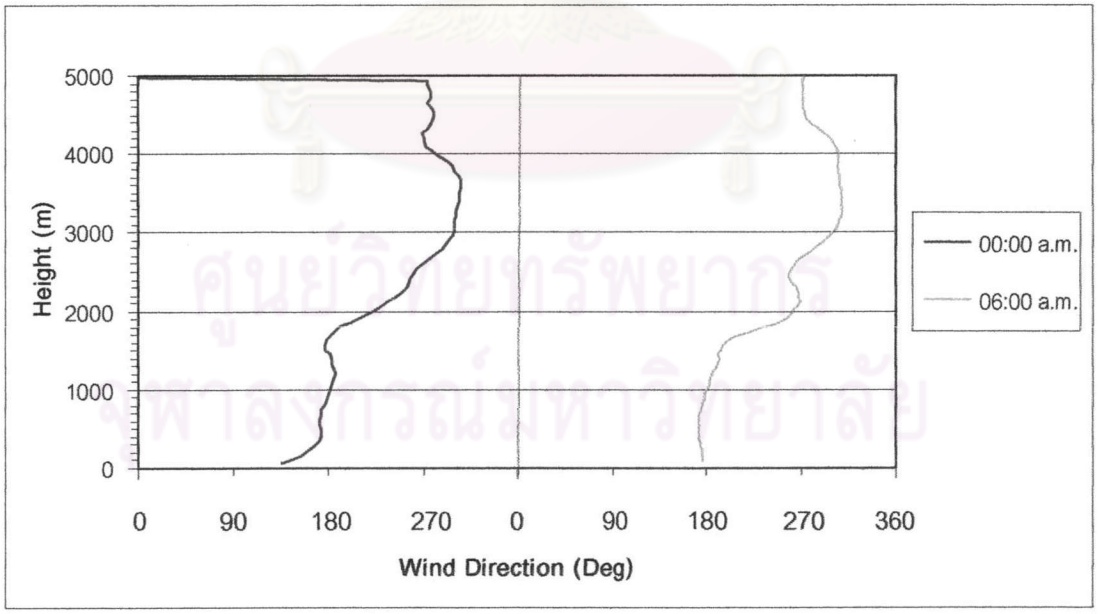


Figure 4.7 Vertical profile of Wind Direction observed during 00:00 a.m. – 06:00 a.m., 23rd January 2002.

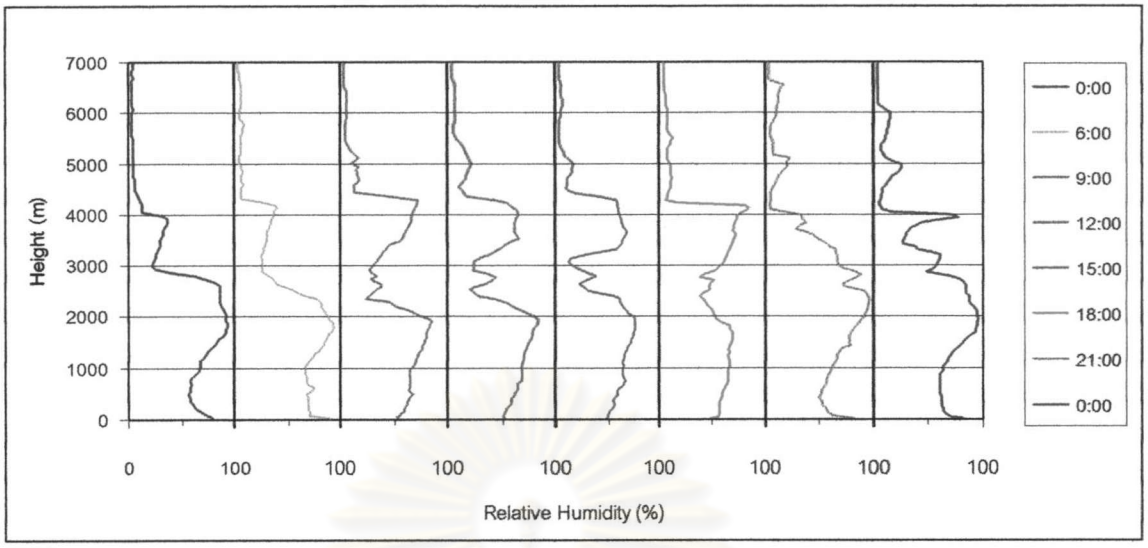


Figure 4.8 Vertical profile of relative humidity observed on 23rd January 2002

**4.2.2.2 Period from 09:00 a.m. to 03:00 p.m.**

In day time, influence of net radiation at the surface generates convection of air mass.

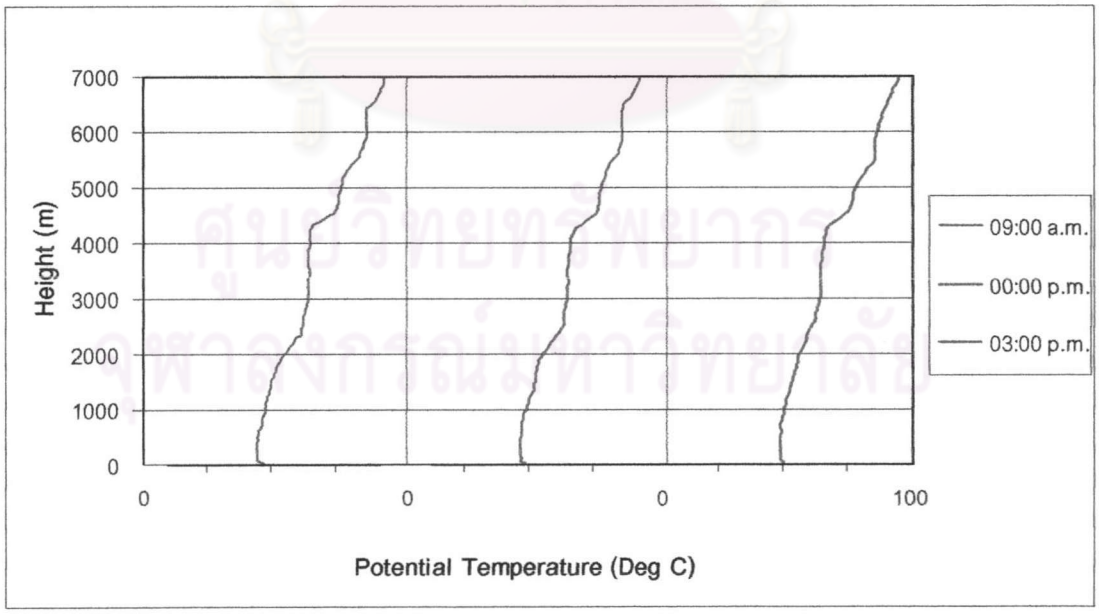


Figure 4.9 Vertical profile of potential temperature observed during 09:00 a.m. – 03:00 p.m., 23rd January 2002.

According to vertical profile of potential temperature, the trend changes at 2 km and 4 km (Figure 4.9). The lower well mixed layer is ABL that overlain by cold and dry air mass (Figure 4.8). Inversion temperature at 2 km is still not clear in vertical profile of temperature data (Figure 4.10).

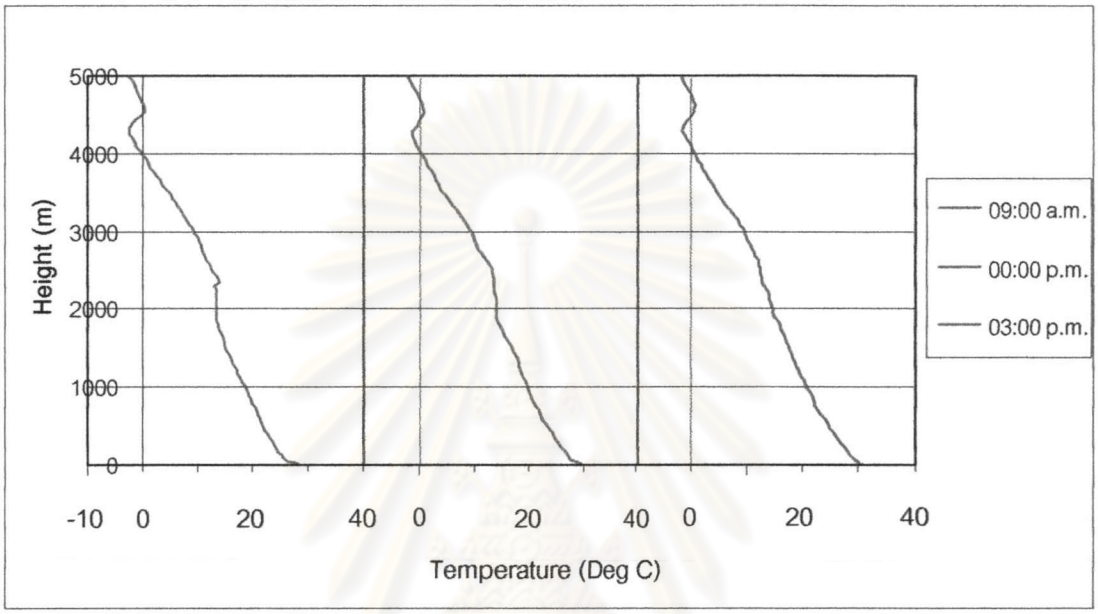


Figure 4.10 Vertical profile of temperature observed during 09:00 a.m. – 03:00 p.m., 23rd January 2002.

Wind directions are the same as before (Figure 4.11). But strong wind speed at 1 km decreased from 09:00 a.m. and disappeared at 15:00 (Figure 4.12). Wind speed is almost constant at 4 m/s from 200 to 1.2 km before it increased continuously at 15:00.

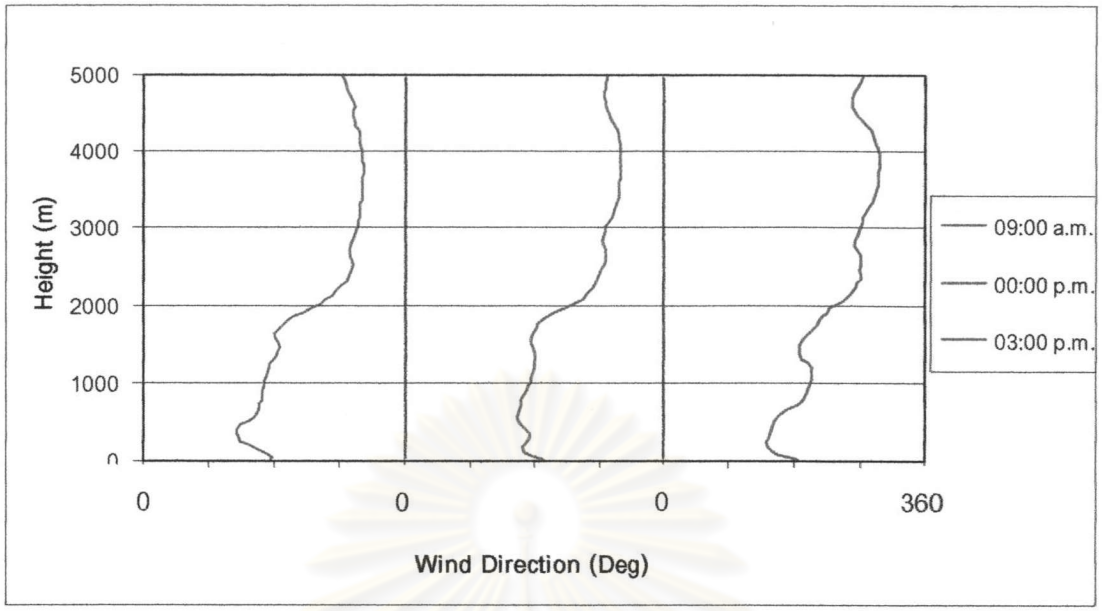


Figure 4.11 Vertical profile of Wind Direction observed during 09:00 a.m. – 03:00 p.m., 23rd January 2002.

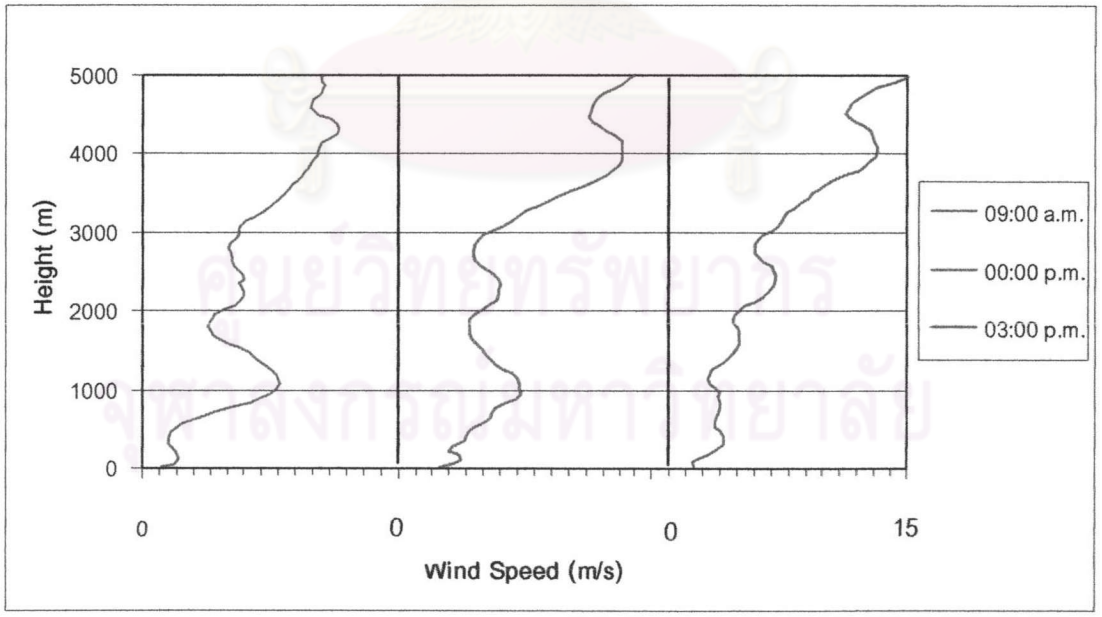


Figure 4.12 Vertical profile of Wind Direction observed during 09:00 a.m. – 03:00 p.m., 23rd January 2002.

#### 4.2.2.3 Period after 03:00 p.m.

According to vertical profile of potential temperature data, the stable layers appear at 1 km and 4 kilometer at 06:00 p.m. Thickness of stable layer at 1 km is about 1.8 km. At 09:00, there are 3 stable layers at near surface, 2.5 km and 4 km (Figure 4.13).

ABL top height is not clear in vertical profile of temperature data (Figure 4.14).

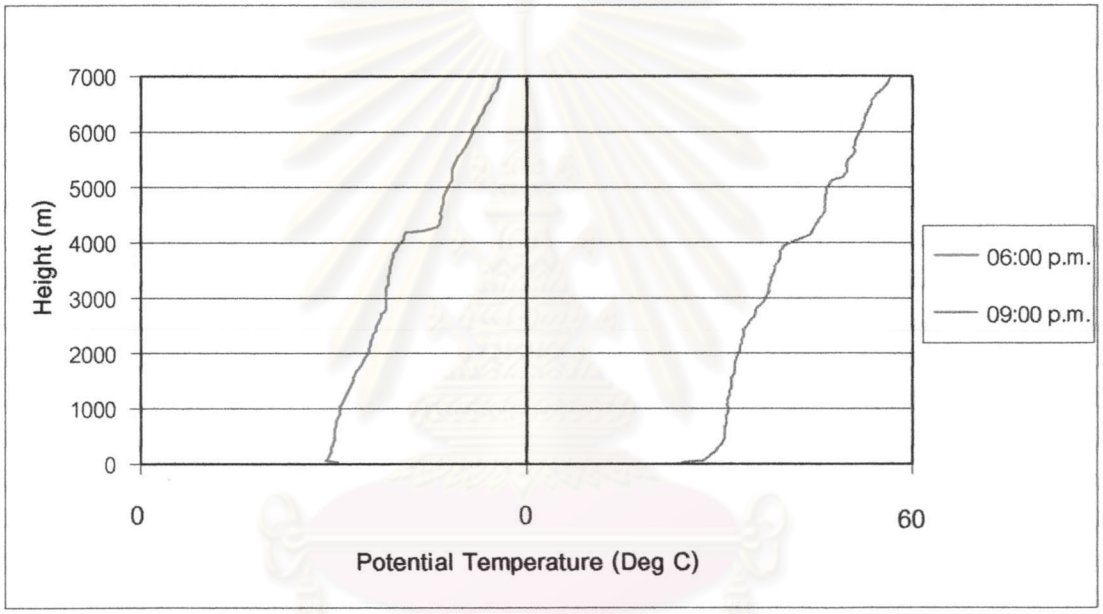


Figure 4.13 Vertical profile of potential temperature observed during 06:00 p.m. – 09:00 p.m., 23rd January 2002.

Wind speed and direction are the same as 06:00 p.m. Although, wind speed continuously increases from surface to 500 m before it increases slowly from 500 m to 3 km (Figure 4.15). Wind direction is south-west wind at surface before change to north wind at 500 m (Figure 4.16).

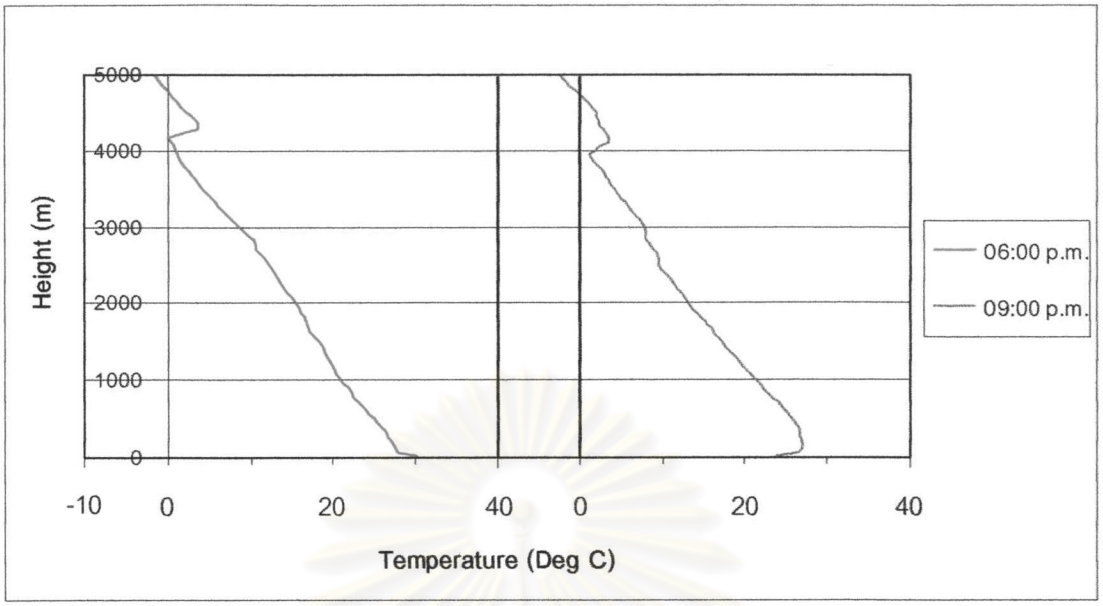


Figure 4.14 Vertical profile of temperature observed during 06:00 p.m. – 09:00 p.m., 23rd January 2002.

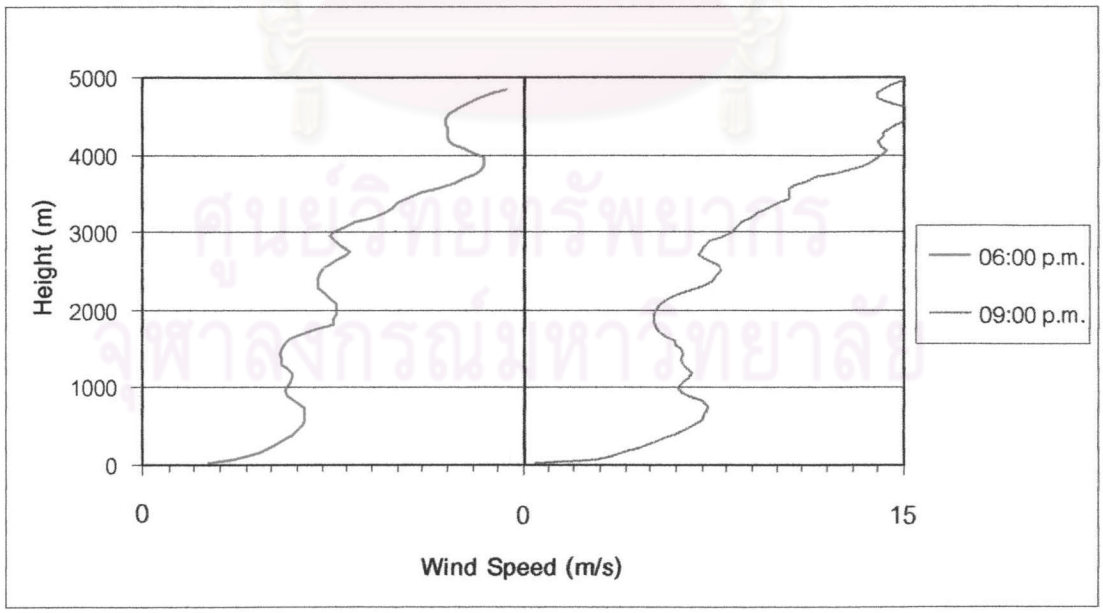


Figure 4.15 Vertical profile of Wind Speed observed during 06:00 p.m. – 09:00 p.m., 23rd January 2002.

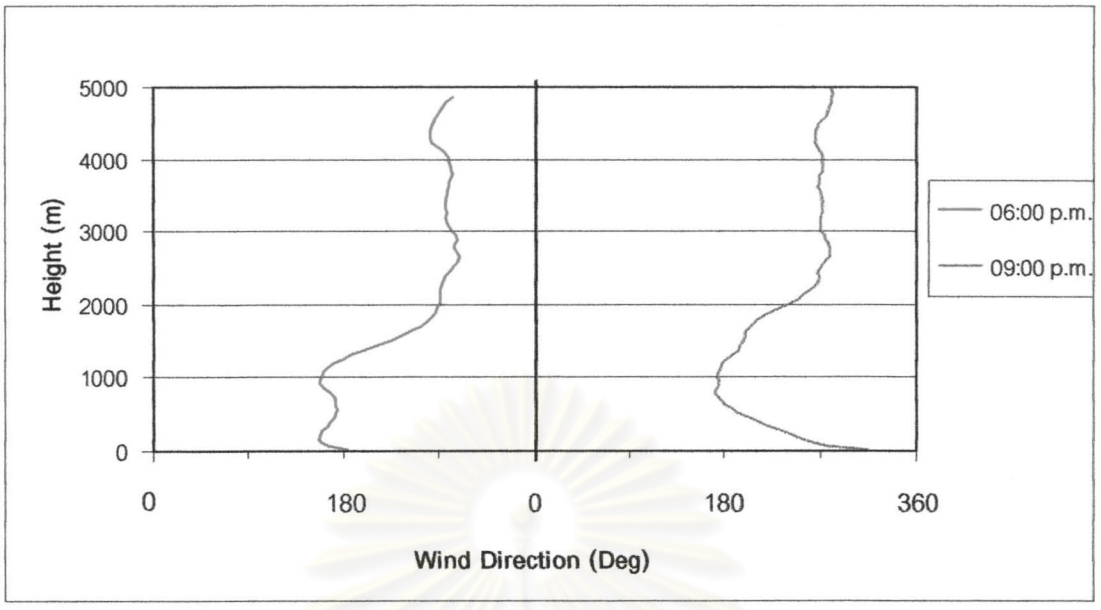


Figure 4.16 Vertical profile of Wind Direction observed during 06:00 p.m. – 09:00 p.m., 23rd January 2002.

### 4.2.3 Lidar data

In 23rd January 2002, backscattering intensity showed two aerosol layers, namely blue layer and yellow layer. Top of ABL is almost constant at 2 km all the day. In addition, the backscattering intensity data shows low aerosol content layer interleave between high aerosol content layers and plume structure that frequently found in Period B. In addition, low aerosol content layer interleaves between high aerosol content layers and convective plume. This kind of structure is frequently formed in Period B. The low aerosol content layer interleave between high aerosol content layers structure occurred from midnight of last day to 06:00 p.m. of 23rd January 2002. Convective plume had been formed before midnight of 23rd January 2002 (Figure 4.17).

According to depolarization ratio data, ABL consist of two kinds of aerosol layers namely high spherical aerosol and low spherical aerosol layer (Figure 4.17).

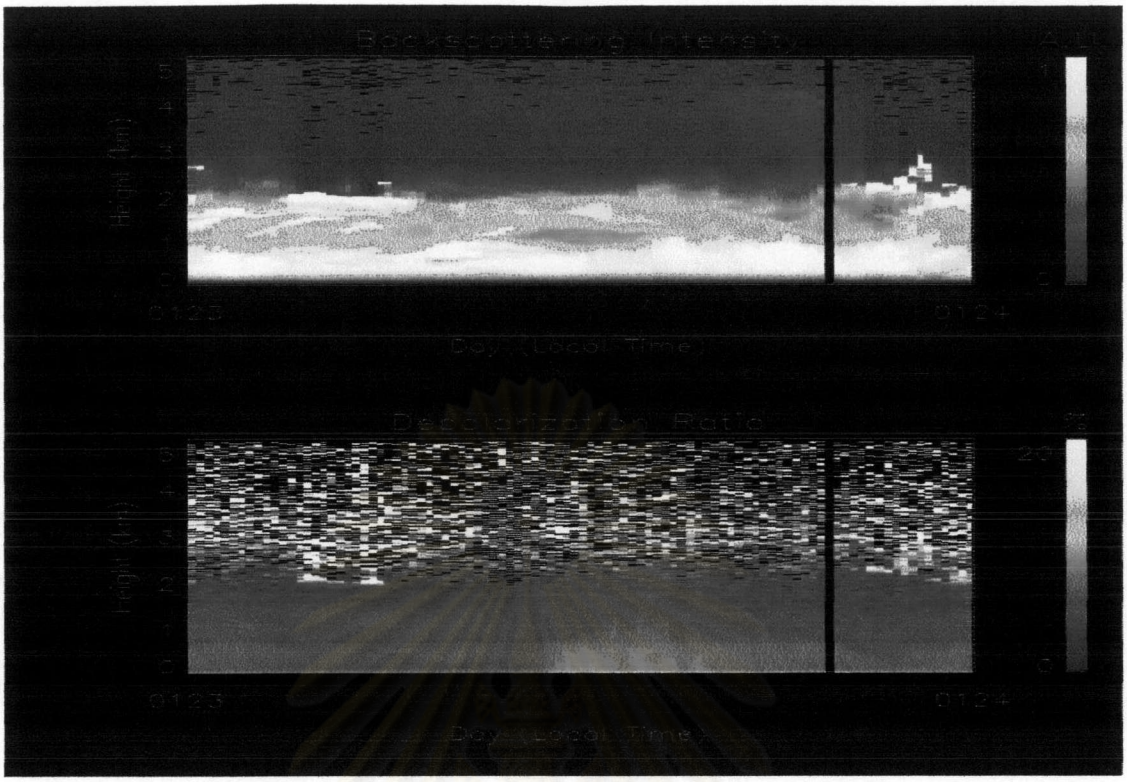

Figure 4.17 Lidar data that observed at 23rd January

Aerosol extinction coefficient data are distinguished into three periods due to the influence of solar radiation, namely, period before 09:00 a.m., period from 09:00 a.m. to 03:00 p.m., and period after 03:00 p.m., following Menut (2000). The aerosol extinction coefficient character of each period described as below;

**4.2.3.1 Period before 09:00 a.m.**

Vertical profile of aerosol extinction coefficient data was divide into three layers, namely, lower high aerosol content layer, low aerosol content layer, and upper high aerosol content layer as describe below.

1) Lower high aerosol content layer, aerosol extinction coefficient is about 2 $\times 10^{-4}$ at surface to 1 km.
2) Low aerosol content layer, aerosol extinction coefficient decreases to 1 $\times 10^{-4}$. Thickness of low aerosol content layer is about 1 km.

3) Upper high aerosol content layer, aerosol extinction coefficient increases from bottom to top of this layer about 1 km. The aerosol extinction coefficient varies from 2 $\times 10^{-4}$ at 00:00 to 4 $\times 10^{-4}$ at 03:00 a.m. and 3$\times 10^{-4}$ at 06:00 a.m. (Figure 4.18).

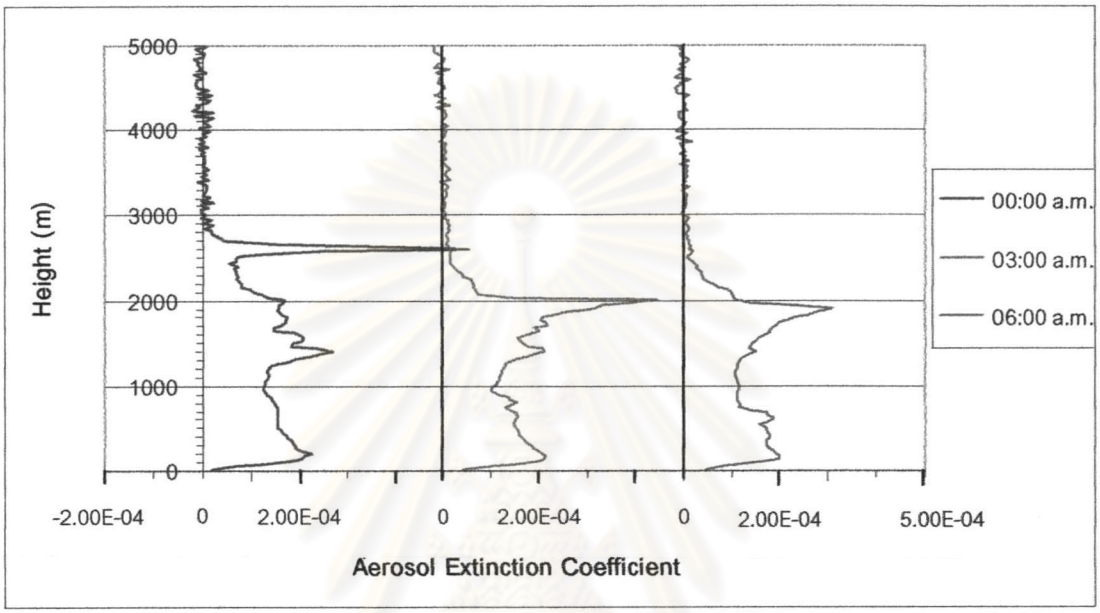


Figure 4.17 Vertical profile of aerosol extinction coefficient observed during 00:00 a.m. – 06:00 a.m., 23rd January 2002.

Aerosol extinction coefficient suddenly decreased at above 2 km and became nearly zero at 2.5 km at 03:00 a.m. to 06:00 a.m. Suddenly increase of aerosol extinction coefficient to 5 $\times 10^{-4}$ At 00:00 a.m., is probably due to error.

**4.2.3.2 Period from 09:00 a.m. to 03:00 p.m.**

The aerosol extinction coefficient of upper and lower high aerosol content layer are about 2 $\times$ $10^{-4}$ from 09:00 a.m. to 00:00 p.m. before upper high aerosol content layer disappears mixed with other layers at 03:00 p.m. (Figure 4.19)

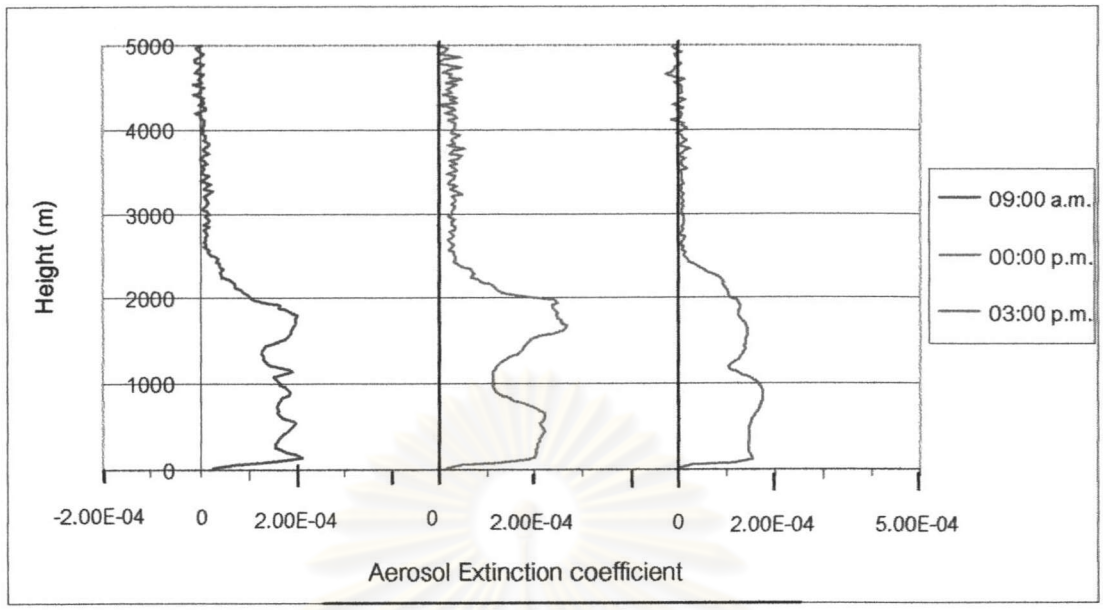


Figure 4.19 Vertical profile of aerosol extinction coefficient observed during 09:00 a.m. – 03:00 p.m., 23rd January 2002.

**4.2.3.3 Period after 03:00 p.m.**

Vertical profile of aerosol extinction coefficient is about $1.7 \times 10^{-4}$ from surface to 1 km. After that, aerosol extinction coefficient is continuously decreased until 2.5 km (Figure 4.20).

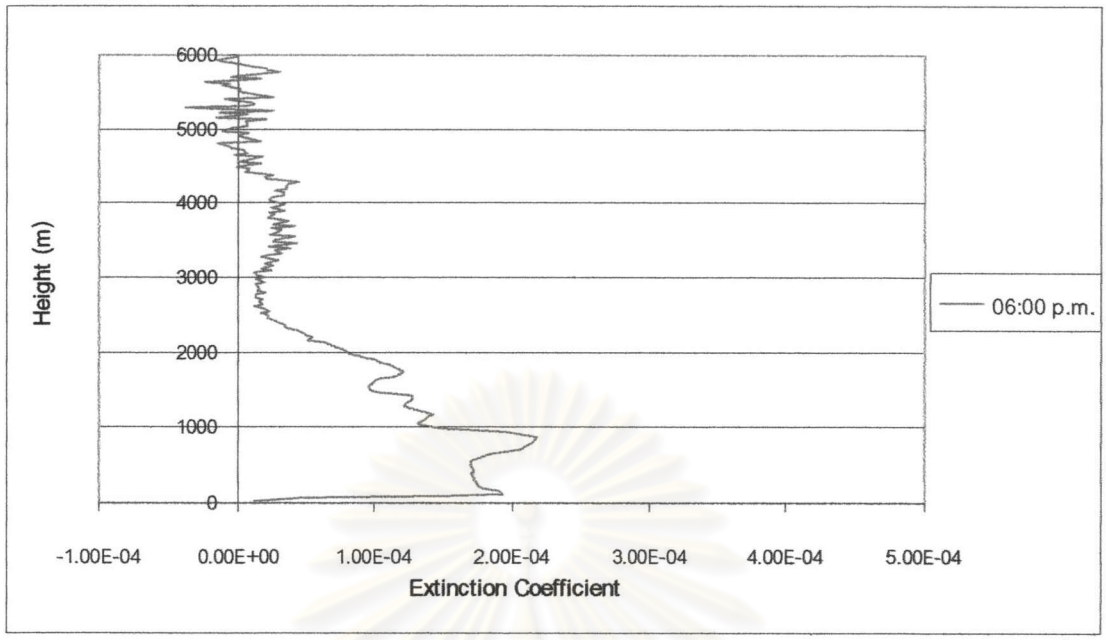


Figure 4.20 Vertical profile of aerosol extinction coefficient observed at 06:00 p.m., 23rd January 2002.

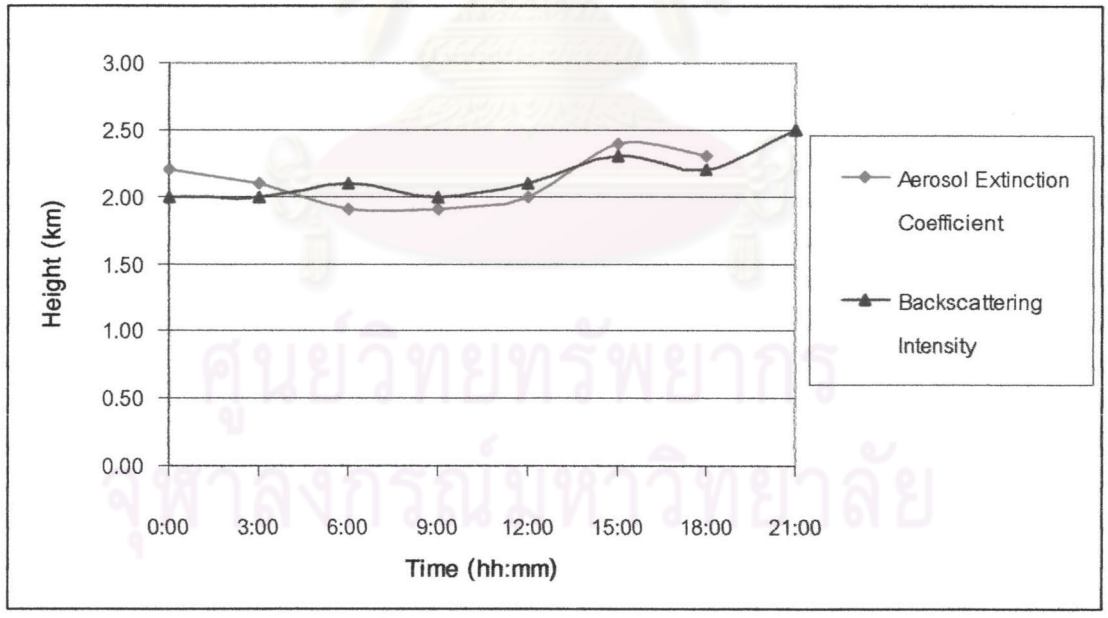


Figure 4.21 ABL top height had identified by backscattering intensity and vertical profile of aerosol extinction coefficient data on 23rd January 2002

ABL top height had been compared by vertical profile of potential aerosol extinction coefficient and backscattering intensity data. The result is ABL top height from both of the data is almost the same (Figure 4.21). In addition, both of lidar data express ABL top height is about 2 – 3 km.

However, according to radiosonde data, ABL compose of high humidity and wind direction is changed at the top of ABL.

## 4.3 Period B (early February to mid May)

Period B covers summer season, starting from February to mid of May. For Period B, the backscattering intensity data shows higher aerosol content than that of the last period, especially at the surface. Plume structure was formed frequently in this period both in day and night time (Figure 4.22). ABL top height increases from 2.5 km at February to 3.5 km at May.

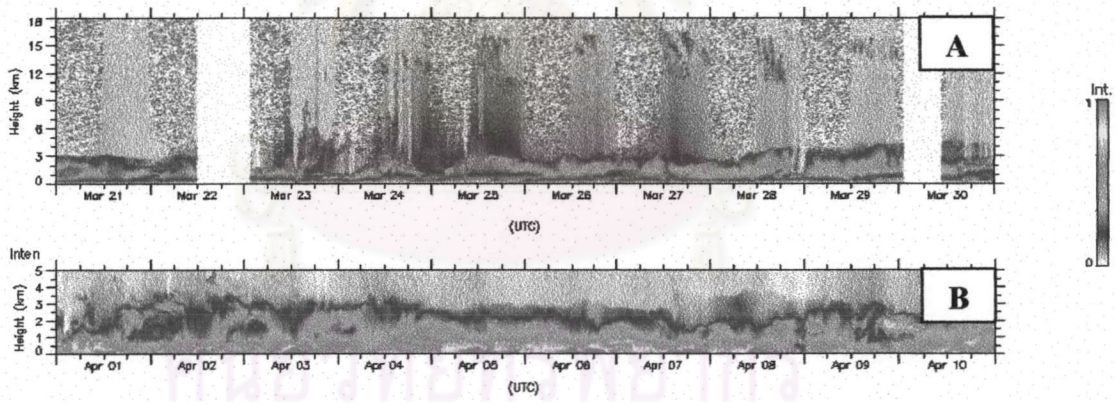


Figure 4.22 An example of backscattering intensity data had been collect in Period B. The data obtained in March 1999 (A) by MPL, and April 2002 (B) by Mie Scattering Lidar.

For period B, radiosonde data were collected during 23rd January – 3rd February 1999, at EGAT tower (70 km west of the Observatory). Radiosondes were launched from 07:00 a.m. to 03:00 p.m. Radiosonde data that collected at 24th February 1999 had been selected as reference data for the analysis assuming ABL was homogeneous. Since

lidar data of 19th April 1999 is MPL, aerosol extinction coefficient does not exist and aerosol content is very low. Therefore data collected in 19th March 2002 have been selected to represent Period B in year 2002.

### 4.3.1 Surface Meteorological data

According to surface meteorological data, pressure is continuously decreased from February to May. The Observatory area is covered by ridge of low pressure. Surface temperature continuously decreased from 27°C at early February to 24°C in early March. In March, temperature was almost constant at average 28.5°C. For April to mid of May, temperature continuously increased to about 30.2°C (Figure 4.23).

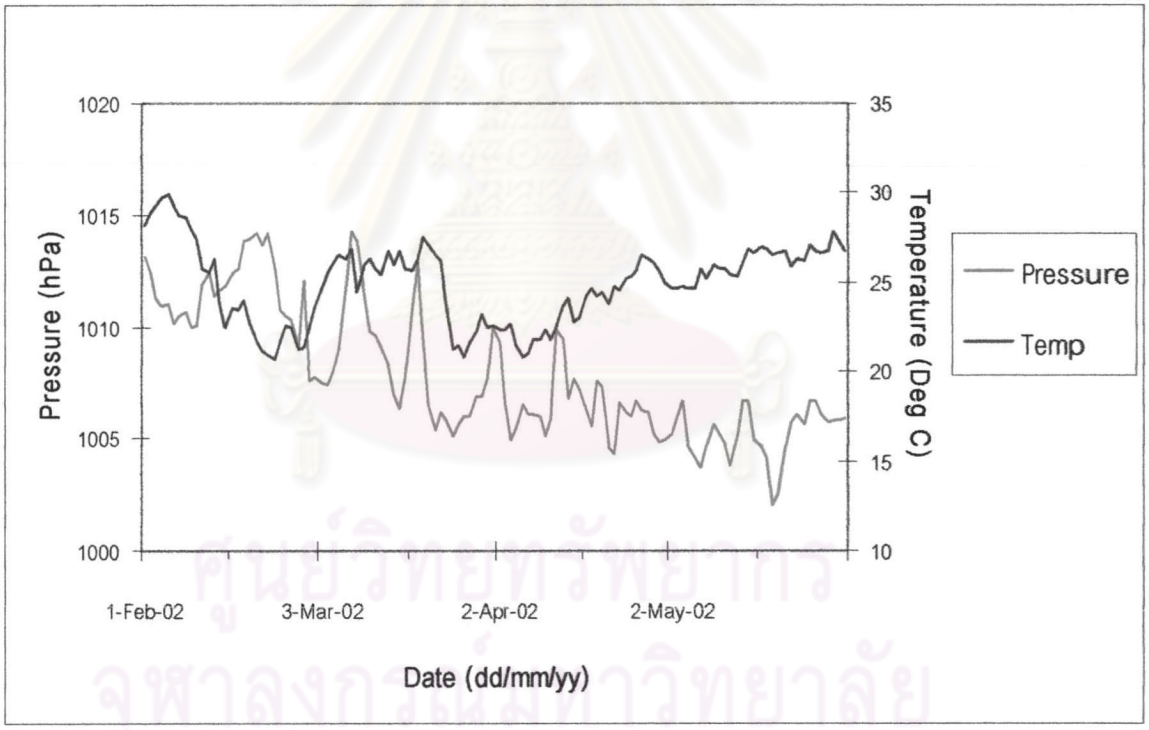


Figure 4.23 Surface pressure and temperature during Period B

According to weather map, ridge of low pressure replaced ridge of high pressure in 24th February 1999. Weather map of 19th March 2002 was similar to that of 24 February 1999 (Figure 4.24 and 4.25).

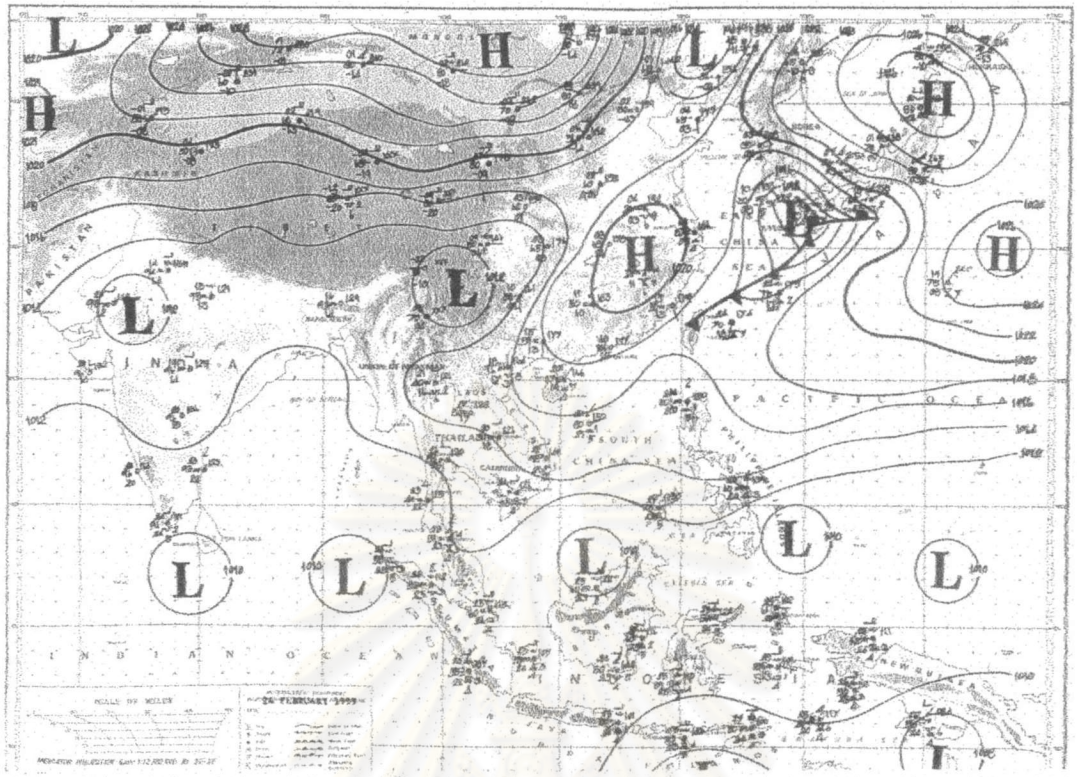


Figure 4.24 Weather map of 24th February 1999

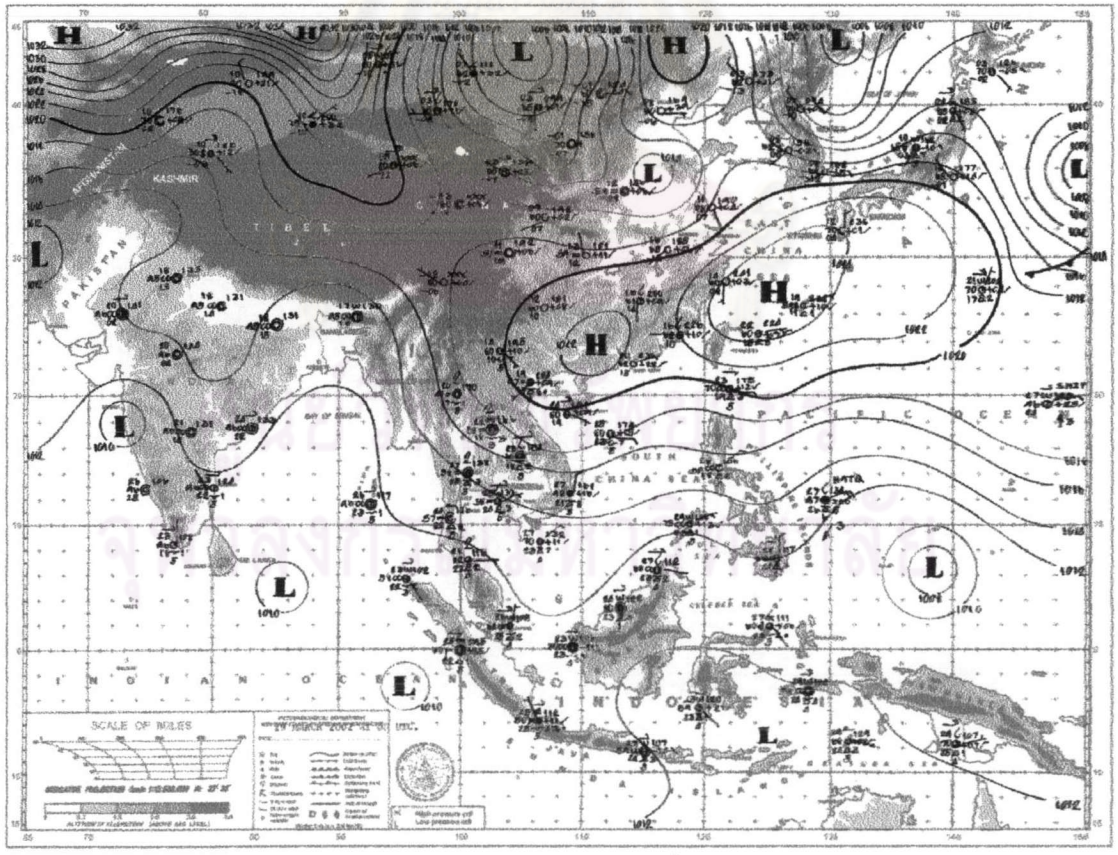


Figure 4.25 Weather map of 19th March 2002

### 4.3.2 Radiosonde data

The vertical profile of potential temperature and temperature shows strong inversion layer at about 3.5 km (Figure 4.26 and 4.27). It corresponds to vertical profile of relative humidity data that also show high humidity at about 3.5 km (Figure 4.28). Vertical profile of relative humidity continuously increased from surface to 3.5 km, indicating dry and cold air mass advection.

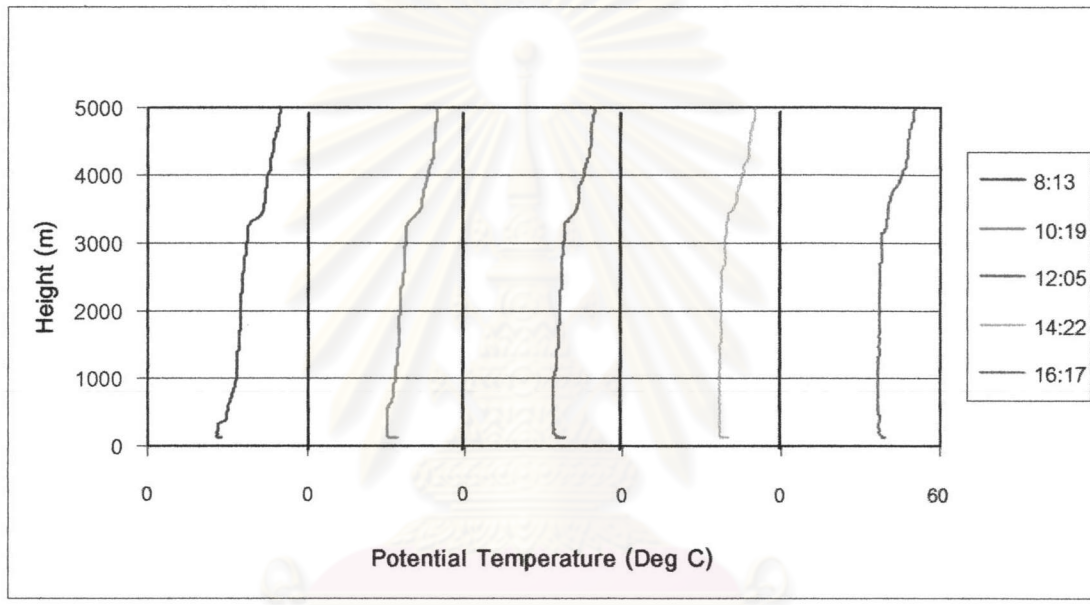


Figure 4.26 Vertical profile of potential temperature observed at 24th February 1999

For vertical profile of wind data, it fluctuates from surface to 5 km. However, strong wind speed is observed at 3 km (Figure 4.28). Wind direction varies from surface to 3 km all the day (Figure 4.29). Above 3 km, wind direction is west wind.

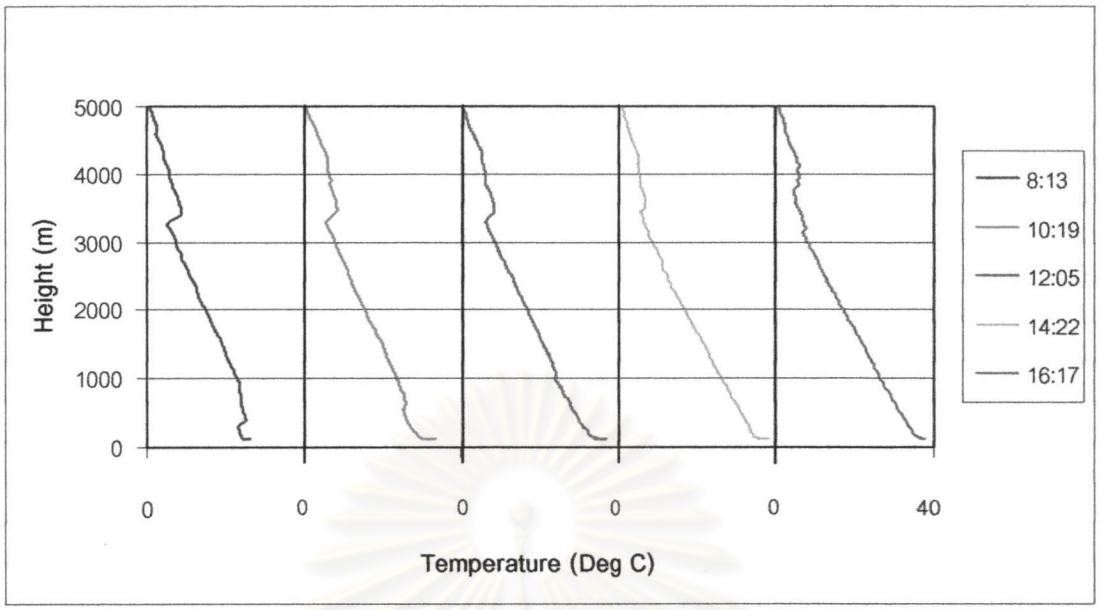


Figure 4.27 Vertical profile of temperature observed on 24th February 1999

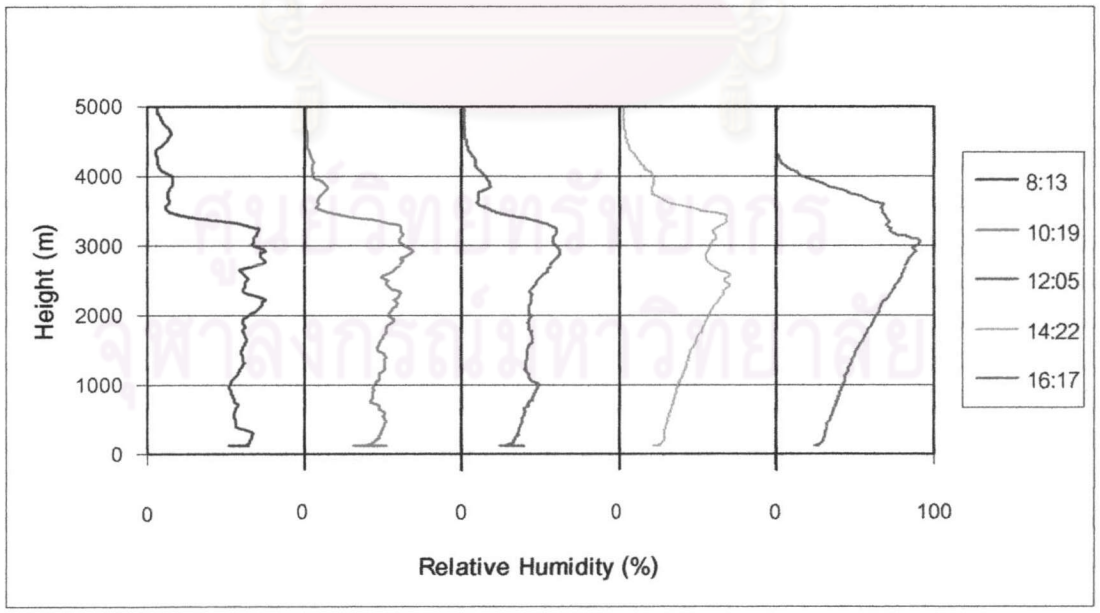


Figure 4.28 Vertical profile of relative humidity observed on 24th February 1999

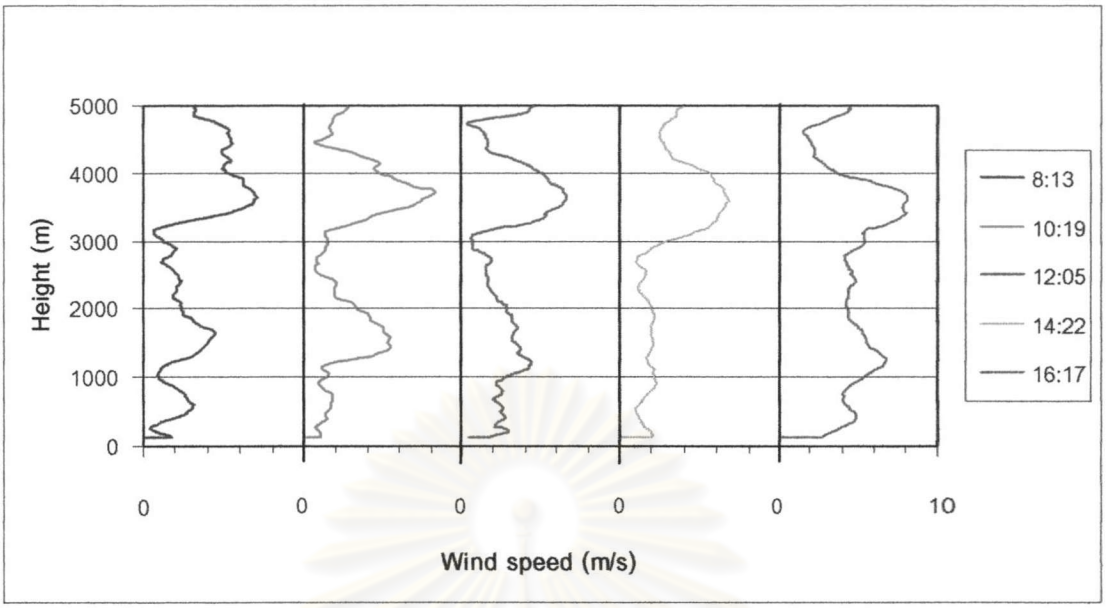


Figure 4.29 Vertical profile of wind speed observed on 24th February 1999

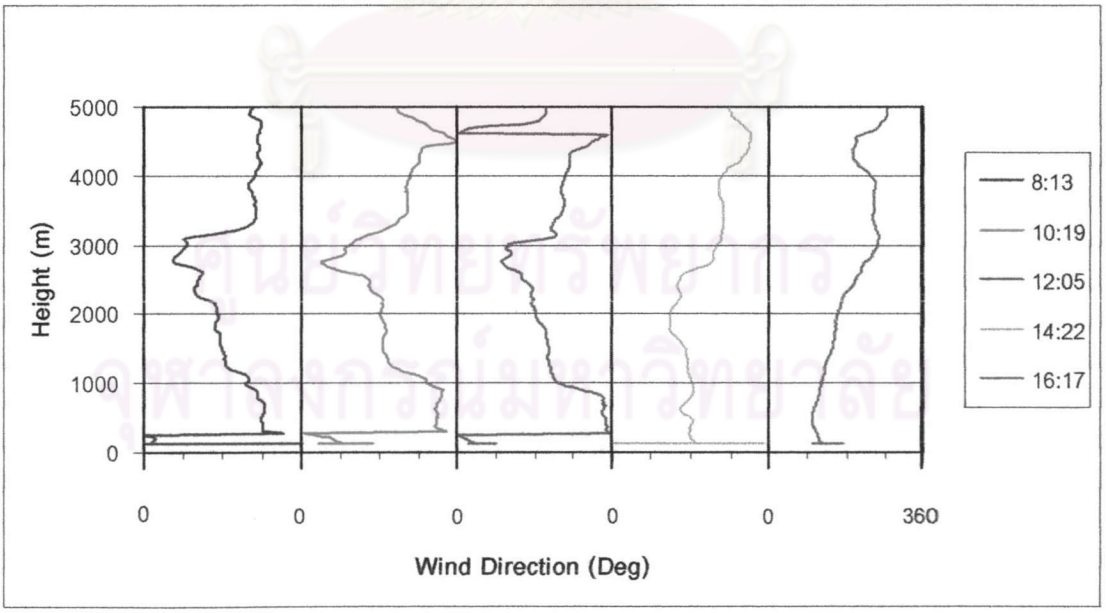


Figure 4.30 Vertical profile of wind direction observed on 24th February 1999

### 4.3.3 Lidar data

Backscattering intensity showed very low aerosol content during 24$^{th}$ – 27$^{th}$ February and high aerosol content layer during 23$^{rd}$ February and 28$^{th}$ February – 3$^{rd}$ March (Figure 4.31).

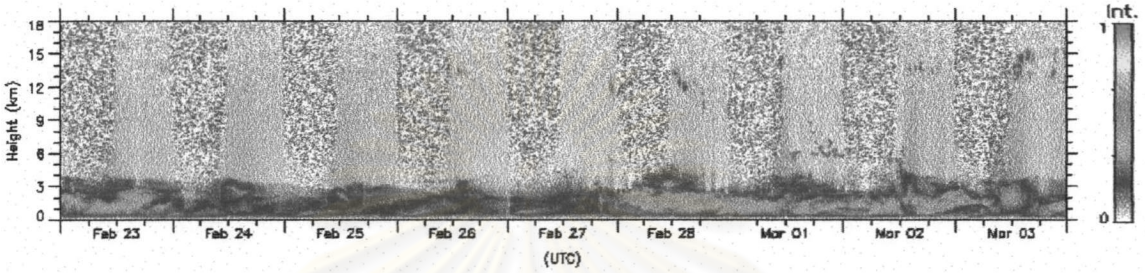


Figure 4.31 Backscattering intensity data collected from 28$^{th}$ February to 3$^{rd}$ March 1999

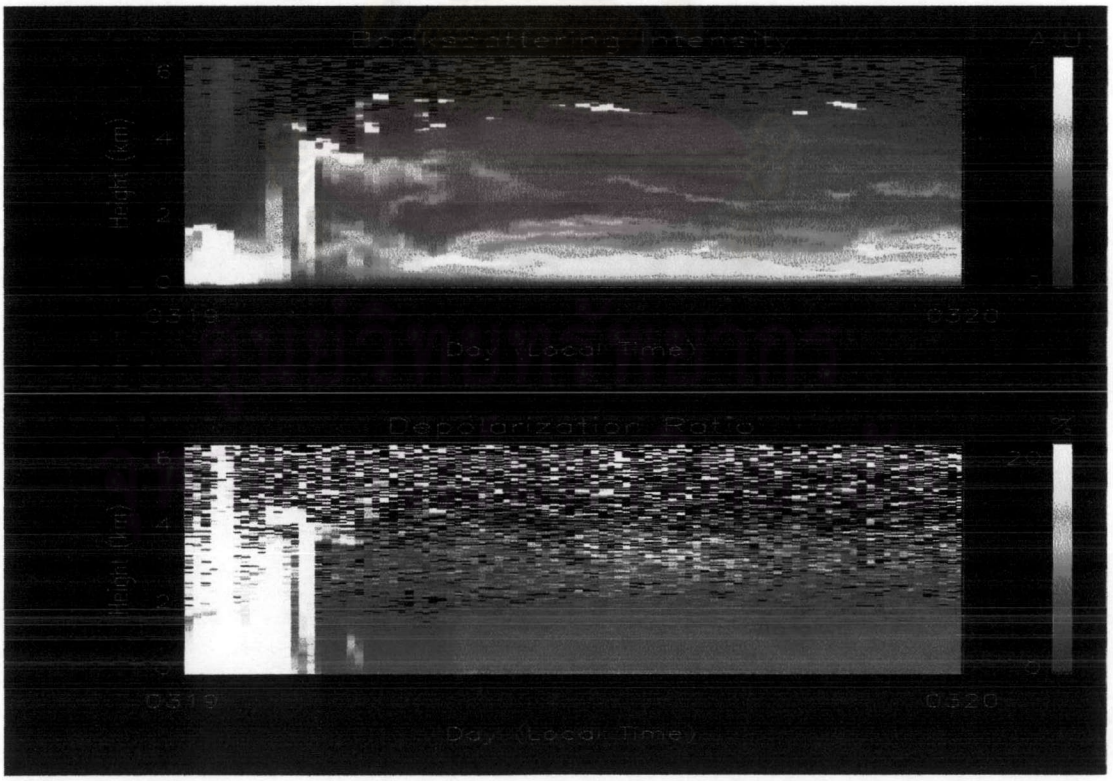


Figure 4.32 Lidar data that observed during 19$^{th}$ March 2002

Backscattering intensity data observed in 19th March 2002, ABL top height is about 5 km. The lower aerosol content layer interleaved between high aerosol content layers structure appeared every day. Therefore lateral wind may prevent ABL formation through the day (Figure 4.31).

The aerosol backscattering intensity data are also divided into three periods following Menut (1999). The aerosol extinction coefficient data showed the same nature, that is, high aerosol extinction coefficient exists near earth surface and it becomes constant before it decreases at 5 km (Figure 4.33, 4.34 and 4.35).

#### 4.3.3.1 Period before 09:00 a.m.

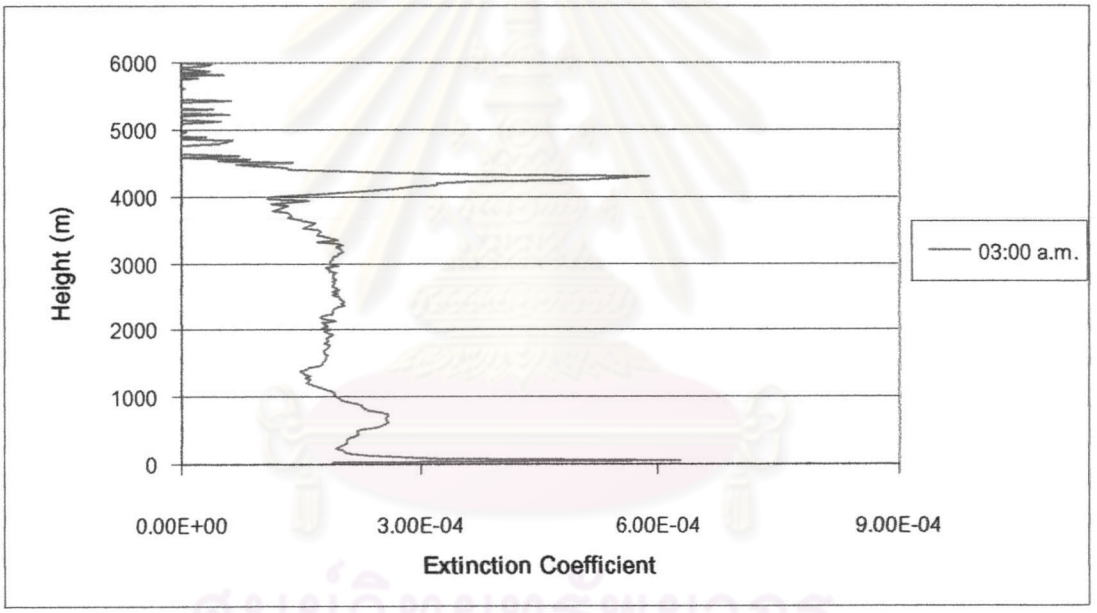


Figure 4.33 Vertical profile of aerosol extinction coefficient observed during 03:00 a.m., 19th March 2002.

#### 4.3.3.2 Period from 09:00 a.m. to 03:00 p.m.

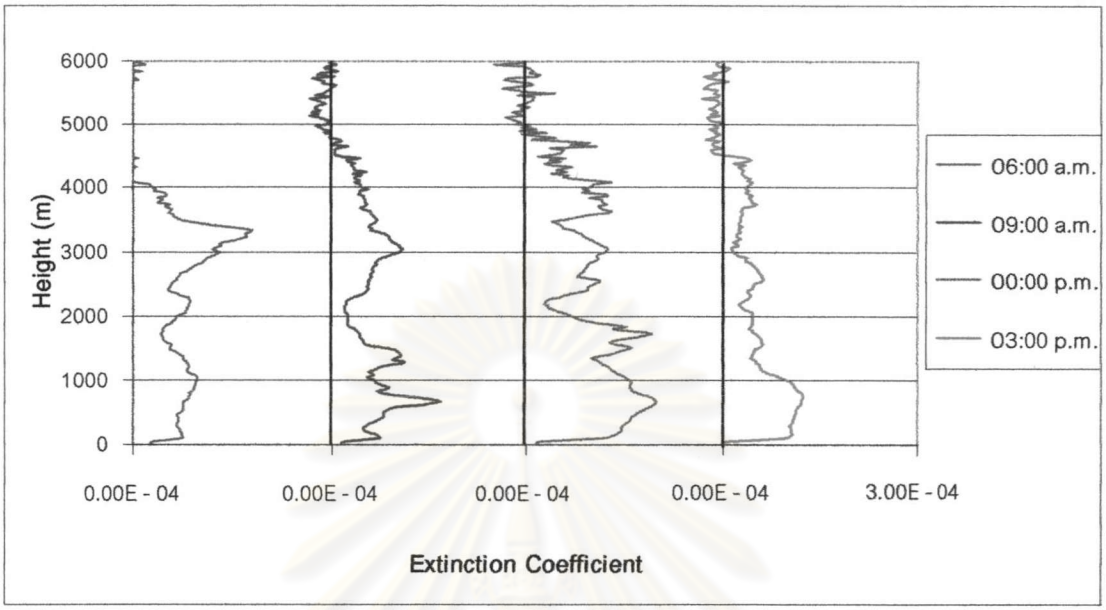


Figure 4.34 Vertical profile of aerosol extinction coefficient observed from 06:00 a.m. to 03:00 p.m., 19th March 2002.

#### 4.3.3.3 Period after 03:00 p.m.

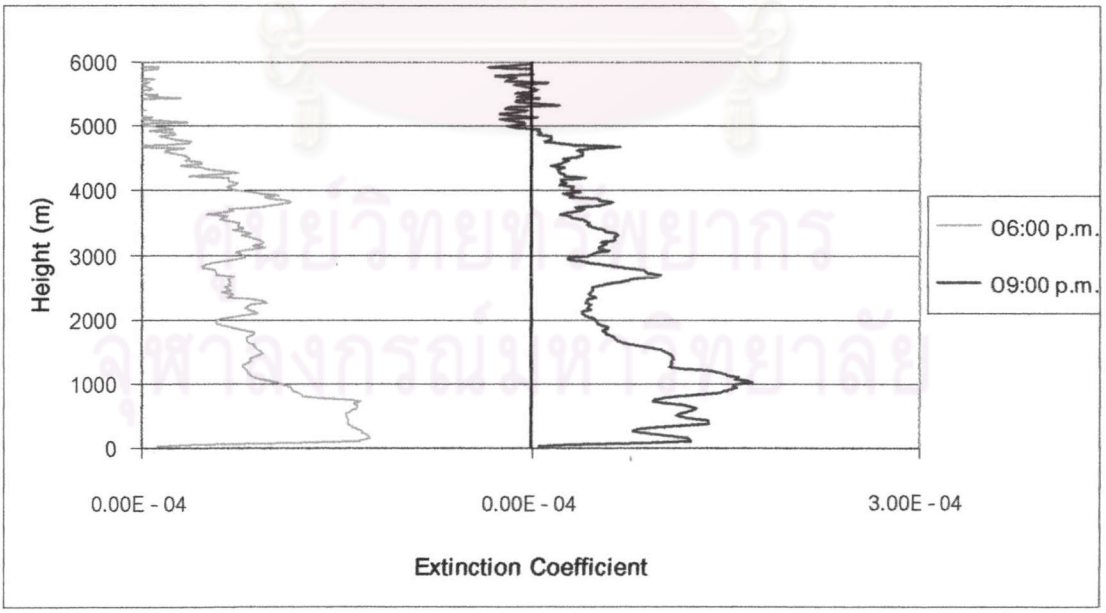


Figure 4.35 Vertical profile of aerosol extinction coefficient observed from 06:00 p.m. to 09:00 p.m., 19th March 2002.

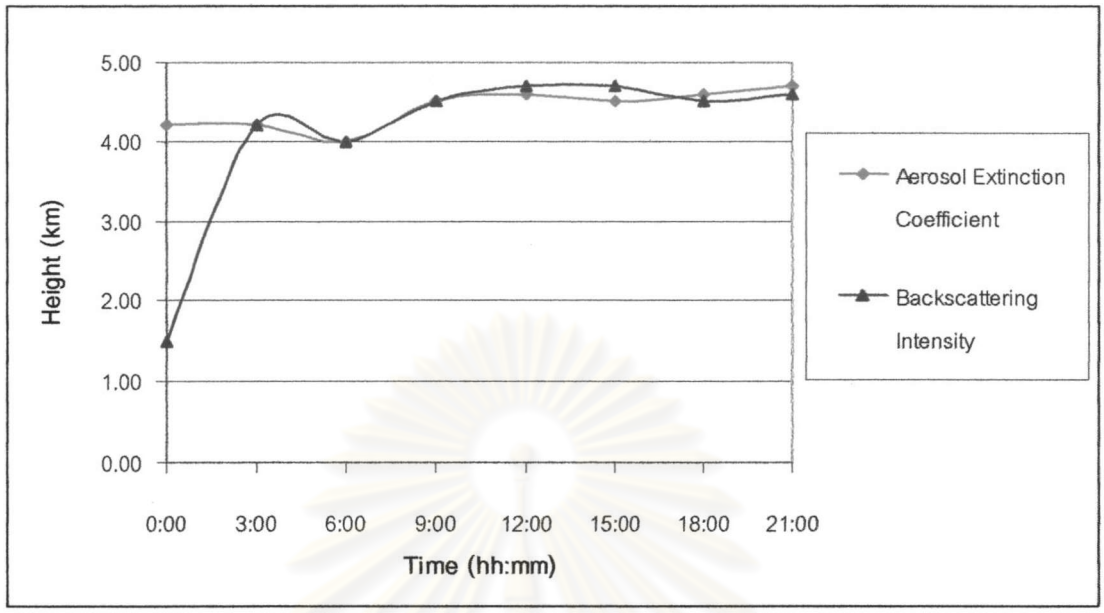


Figure 4.36 ABL top height had identified by backscattering intensity and vertical profile of aerosol extinction coefficient data on 19th March 2002

According to Figure 4.35, ABL top height is almost the same when identified by backscattering intensity and aerosol extinction coefficient data. Top of ABL is about 4.5 km on 19th March 2002.

## 4.4 Period C (mid May to early November)

Period C starts from mid May to early November, covering rainy season. According to surface meteorological data, the low pressure covers Thailand during this period. Therefore cloud covers the Observatory every day in backscattering intensity data. The backscattering intensity data showed aerosol content decreased from early Period C and it almost disappears in later part of this period (Figure 4.37).

The data that collected in 26$^{th}$ October 2001 had been selected to represent Period C.

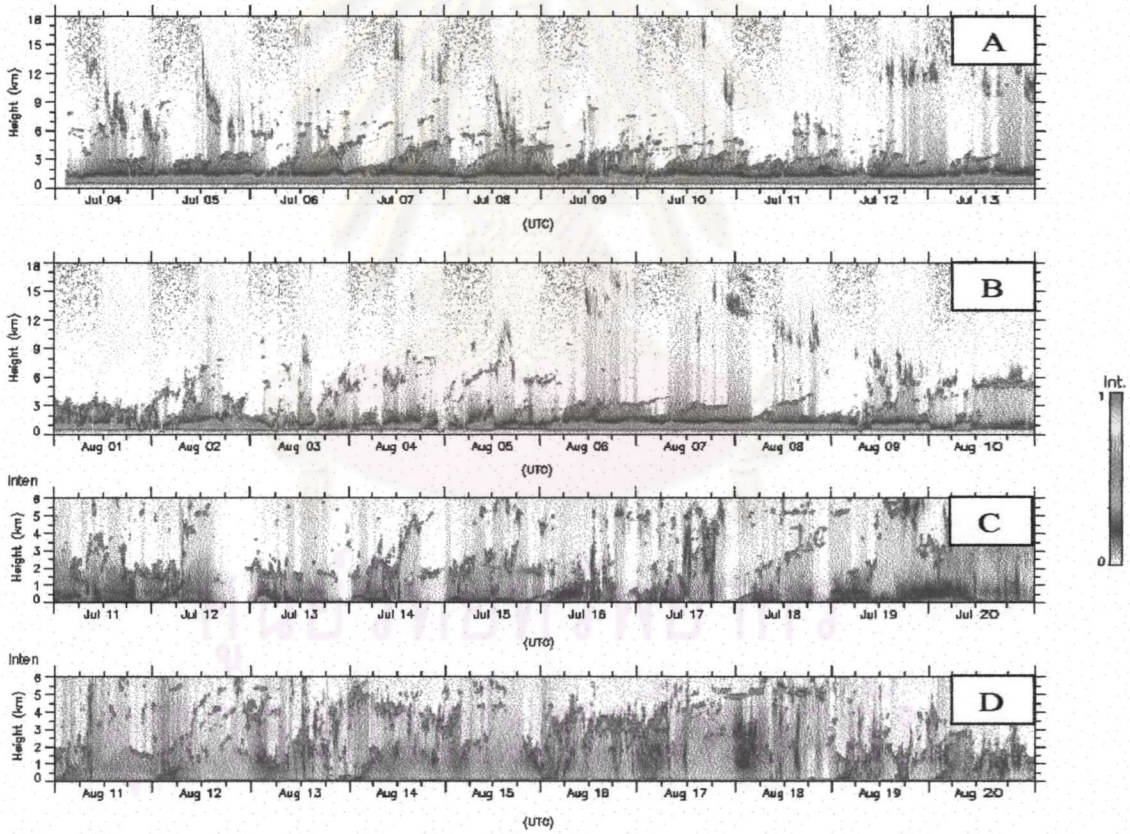


Figure 4.37 The backscattering intensity data had been collected in Period C. The data obtained at June (A), and August 1997 (B) by MPL, July (C) and August 2002 (D) by Mie Scattering Lidar.

### 4.4.1 Surface Meteorological data

According to surface meteorological data, temperature varied from 26°C – 29°C and average temperature was 28.5°C. Surface pressure increased from 1001.6 hPa in May to 1008.5 hPa in October (Figure 4.38).

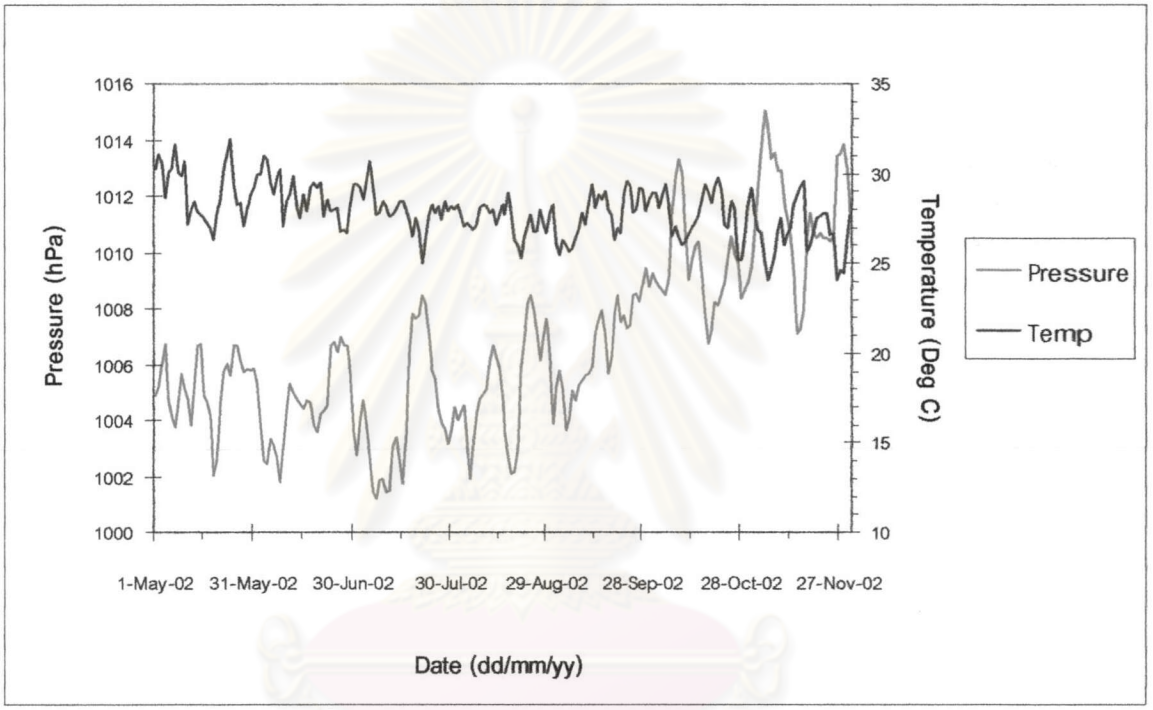


Figure 4.38 Surface pressure and temperature during Period C

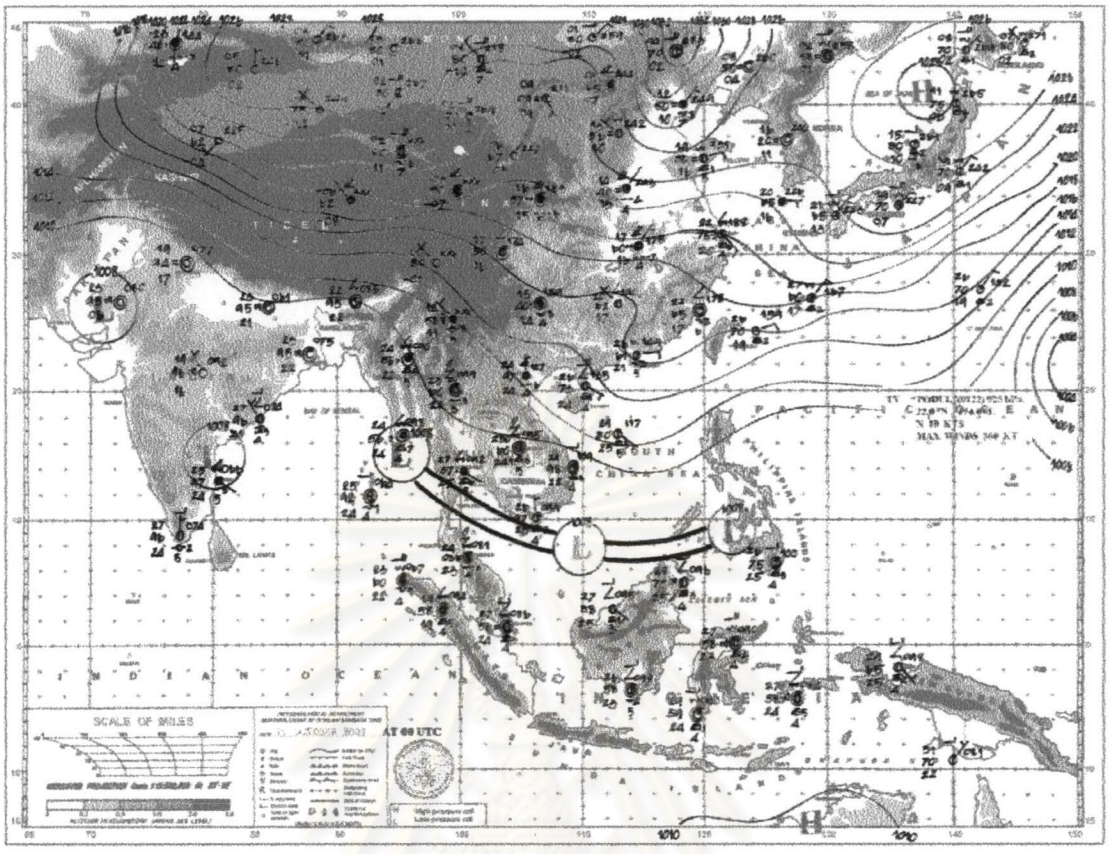

Figure 4.39 Weather map of 27th October 1999

### 4.4.2 Radiosonde data

In Period C, radiosonde data were obtained in two periods, namely 25th – 28th October 2001 and 28th – 30th June 2002. Radiosonde data that collected at 27th October 2001 had been selected to represent Period C.

#### 4.4.2.1 Period before 09:00 a.m.

According to vertical profile of potential temperature, stable layer is formed near the surface and top of ABL is at 2 km at 00:00 a.m. After that, top of stable layer increased to about 400 m and top of ABL is about 3 km at 03:00 a.m. (Figure 4.40). For vertical profile of wind data, wind direction changed from south at surface to north at 1 km before it changed slowly to west at 4 km (Figure 4.41). According to vertical profile of

wind direction data, stable layer at surface is formed by influence of mechanical convection. Wind speed varied from surface to about 3 km at 00:00 a.m. and 2 km at 03:00 a.m. (Figure 4.42). Vertical profile of relative humidity is about 80% and quite constant from surface (Figure 4.49).

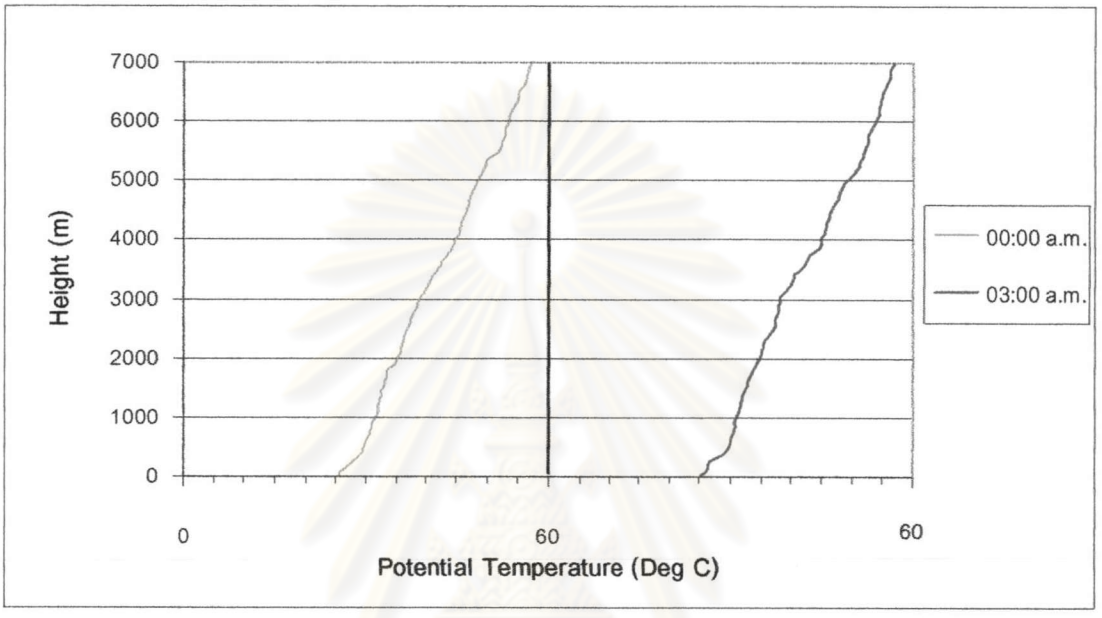


Figure 4.40 Vertical profile of Potential Temperature observed at 00:00 a.m. and 03:00 a.m., 27th October 2001.

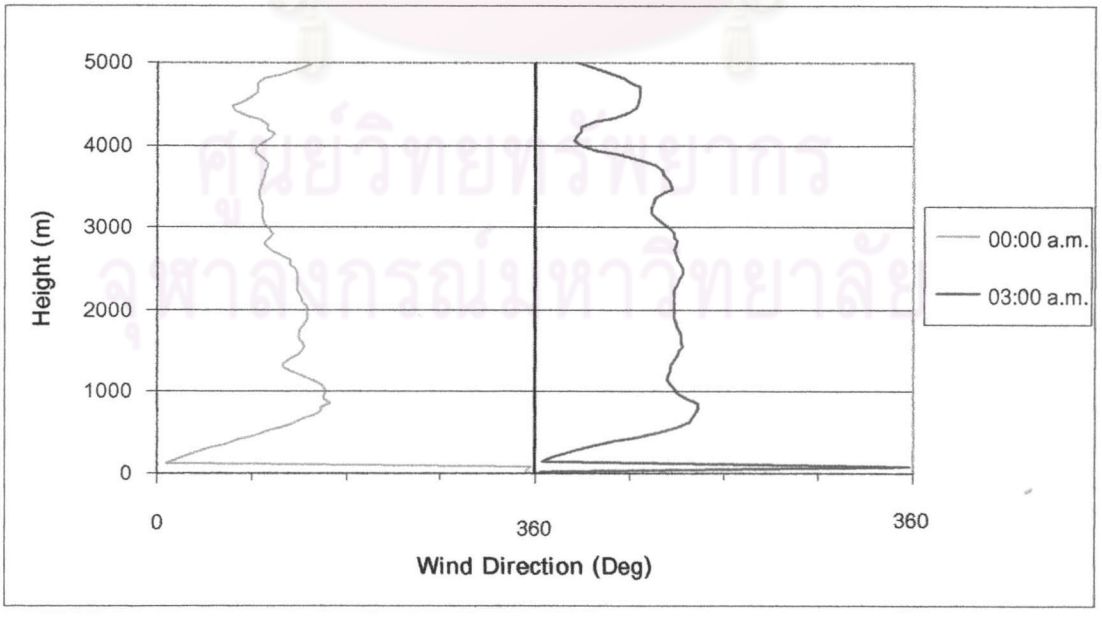


Figure 4.41 Vertical profile of wind direction observed at 00:00 a.m. and 03:00 a.m., 27th October 2001.

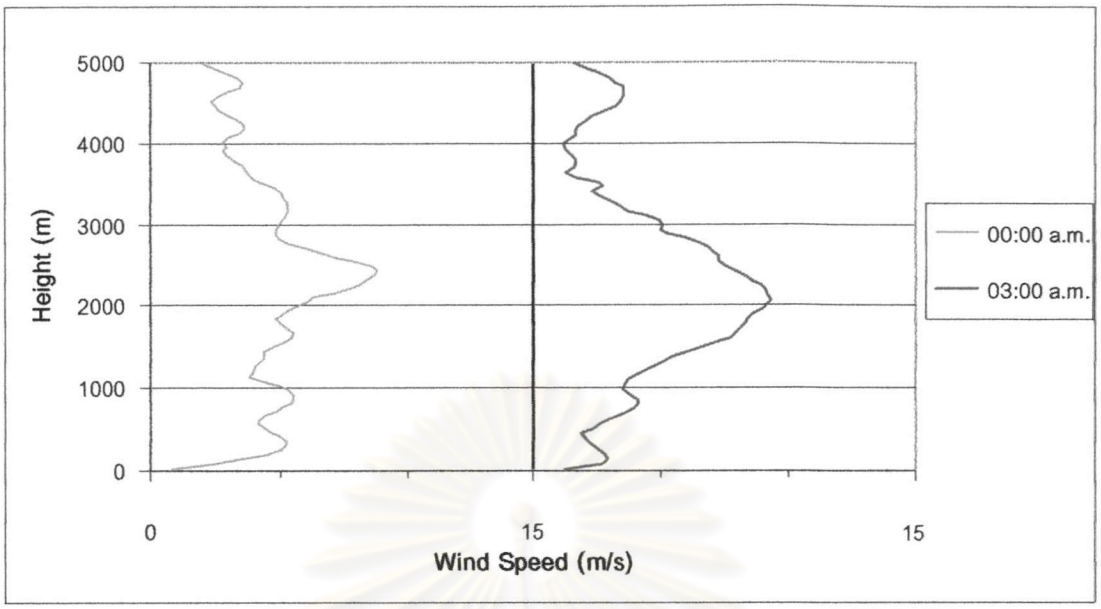


Figure 4.42 Vertical profile of wind speed observed at 00:00 a.m. to 03:00 a.m., 27th October 2001.

**4.4.2.2 Period from 06:00 a.m. to 03:00 p.m.**

Stable layer near the surface still occurred at 06:00 a.m. before it increased from 500 m at 09:00 a.m. to 1 km at 00:00 a.m. Vertical profile of potential temperature increased continuously (Figure 4.43).

Wind direction is the same as before near surface, that is south wind. After that it slowly changed from south to north-east (Figure 4.44). Wind speed increased to 5 m/s near surface at 06:00 a.m. The stable layer near surface is formed by this wind. After that, wind speed is almost constant before it increased at 500 m at 09:00 a.m. and 800 m at 00:00 p.m. (Figure 4.45).

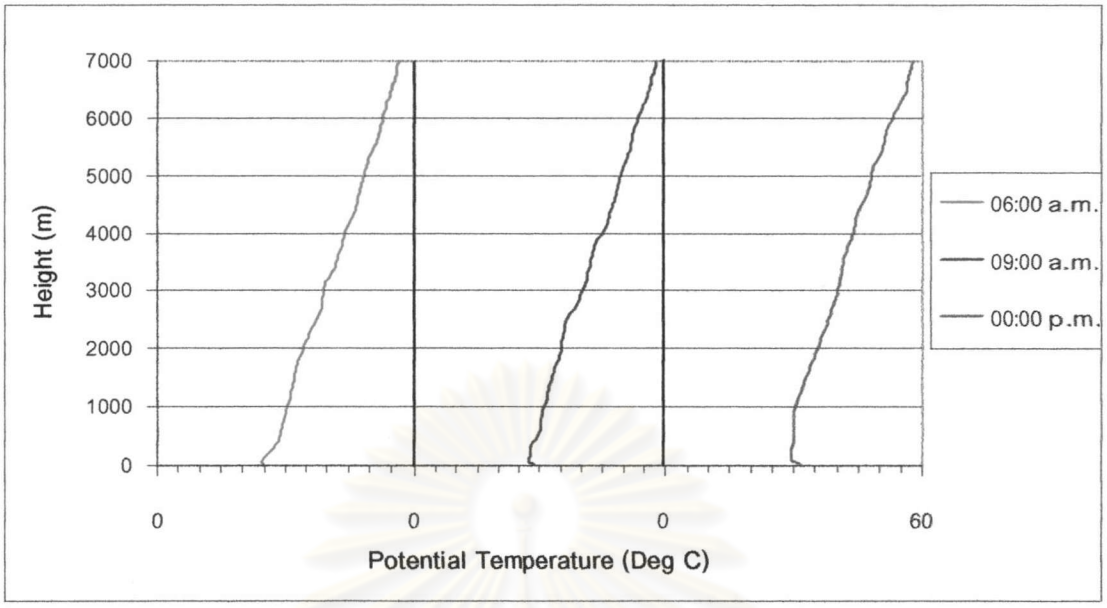


Figure 4.43 Vertical profile of Potential Temperature observed during 06:00 a.m. to 00:00 p.m., 27th October 2001.

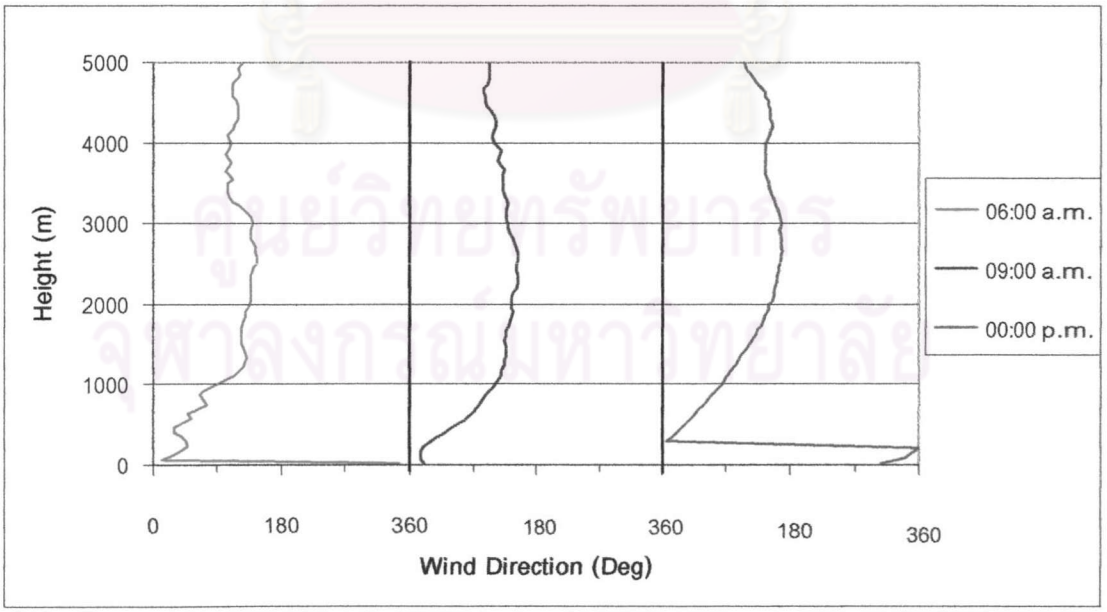


Figure 4.44 Vertical profile of Potential Temperature observed during 06:00 a.m. to 00:00 p.m., 27th October 2001.

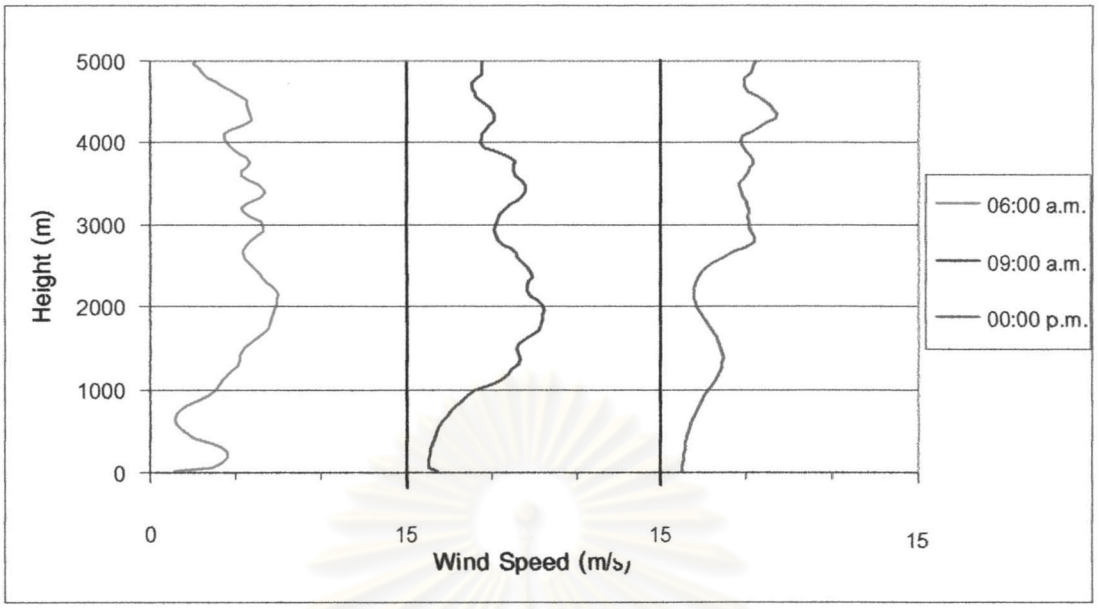


Figure 4.45 Vertical profile of Potential Temperature observed during 06:00 a.m. to 00:00 p.m., 27th October 2001.

**4.4.2.3 Period after 03:00 p.m.**

The vertical profile of potential temperature and wind speed is the same between 00:00 p.m. to 03:00 p.m. (Figure 4.46 and 4.48). However, wind direction slowly changed from north at surface to south west (Figure 4.47). After that, stable layer is formed near surface between 06:00 p.m. and 09:00 p.m. (Figure 4.46). Wind direction varied at surface from north at 06:00 p.m. to south at 09:00 p.m. but wind speed is the same (Figure 4.48).

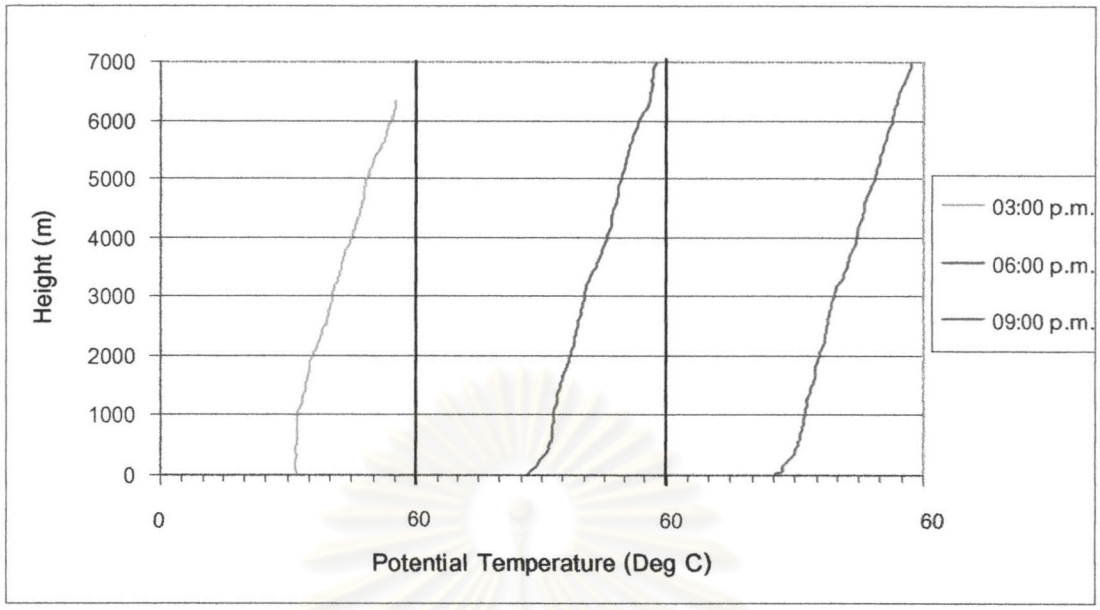


Figure 4.46 Vertical profile of Potential Temperature observed during 03:00 p.m. to 09:00 p.m., 27th October 2001.

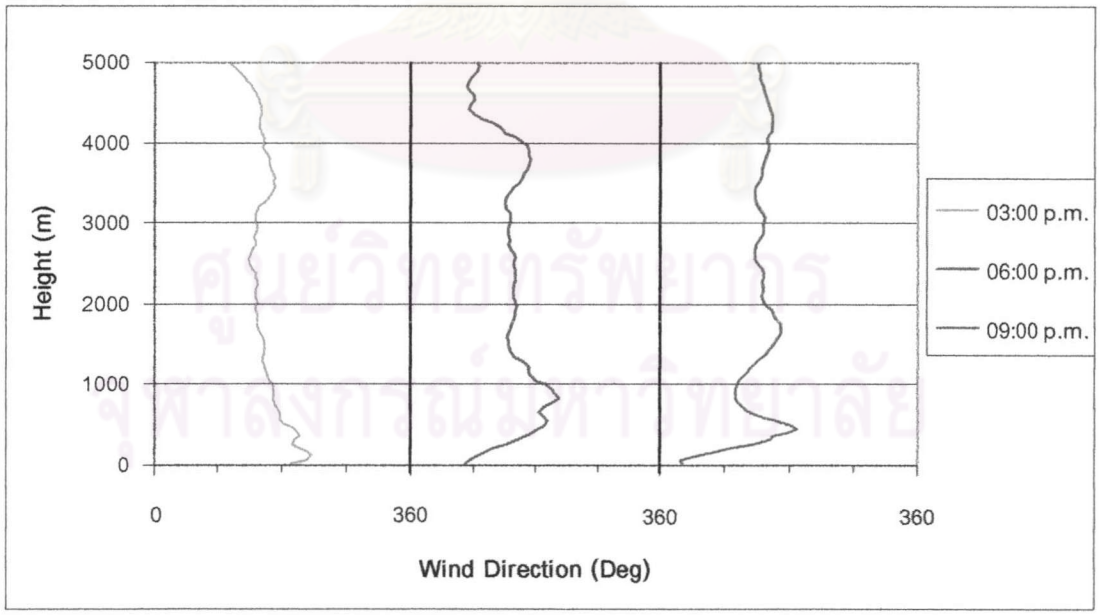


Figure 4.47 Vertical profile of wind direction observed during 03:00 p.m. to 09:00 p.m., 27th October 2001.

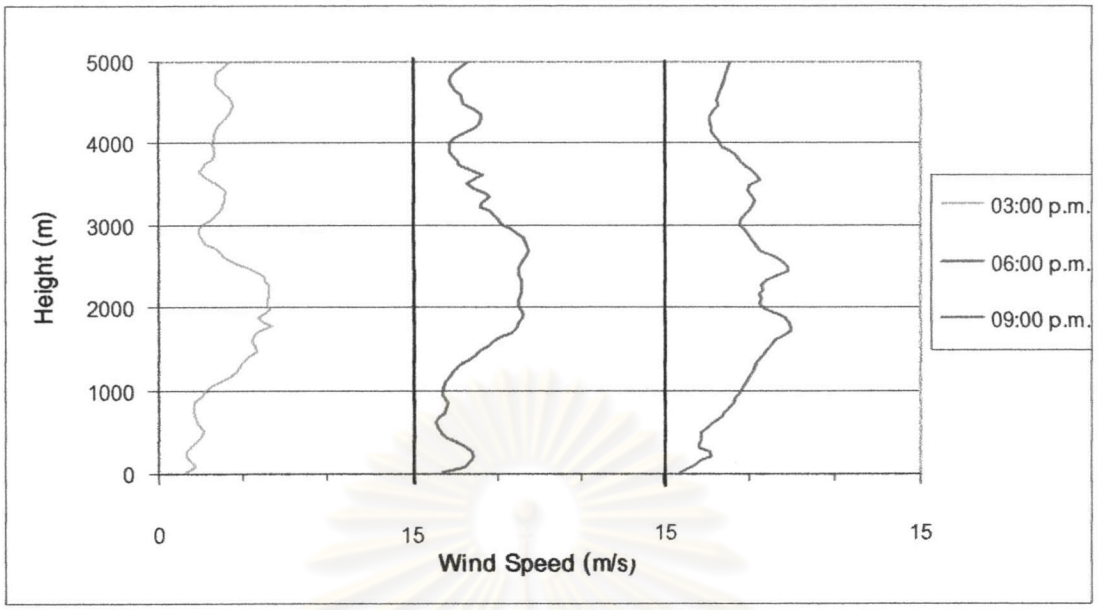


Figure 4.48 Vertical profile of wind speed observed during 03:00 p.m. to 09:00 p.m., 27th October 2001.

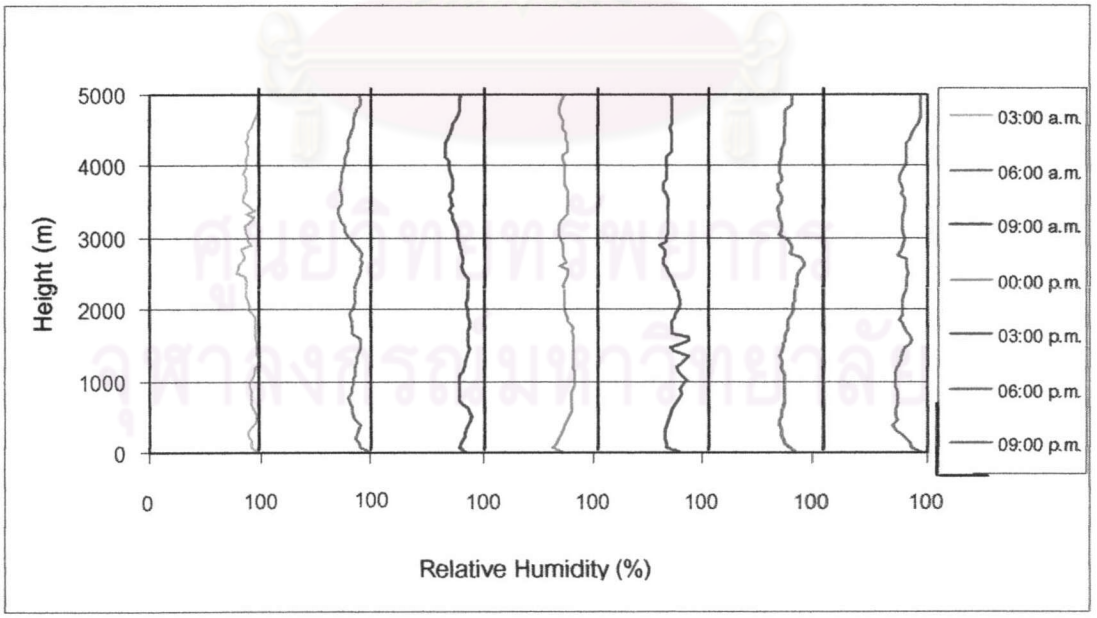


Figure 4.49 Vertical profile of relative humidity observed at 27th October 2001

### 4.4.3 Lidar data

According to backscattering intensity data, ABL is a red layer that is formed under cloud base (white layer). ABL developed under cloud base from a few hundred meters at 09:00 a.m. to 2 km at 03:00 p.m. About 05:00 p.m., the cloud disappears and ABL top height drops to 1 km. After 06:00 p.m., the cloud appears again and ABL rises up to 2 km to form convective plume and top of plume is still under the cloud base (Figure 4.50).

Depolarization ratio data shows ABL diurnal variation is caused by low spherical aerosol under the cloud base but the low spherical layer decay and finally disappeared at the time when ABL top height dropped to 1 km. After that the high spherical aerosol layer was formed, probably due to wind direction changed at 03:00 p.m.

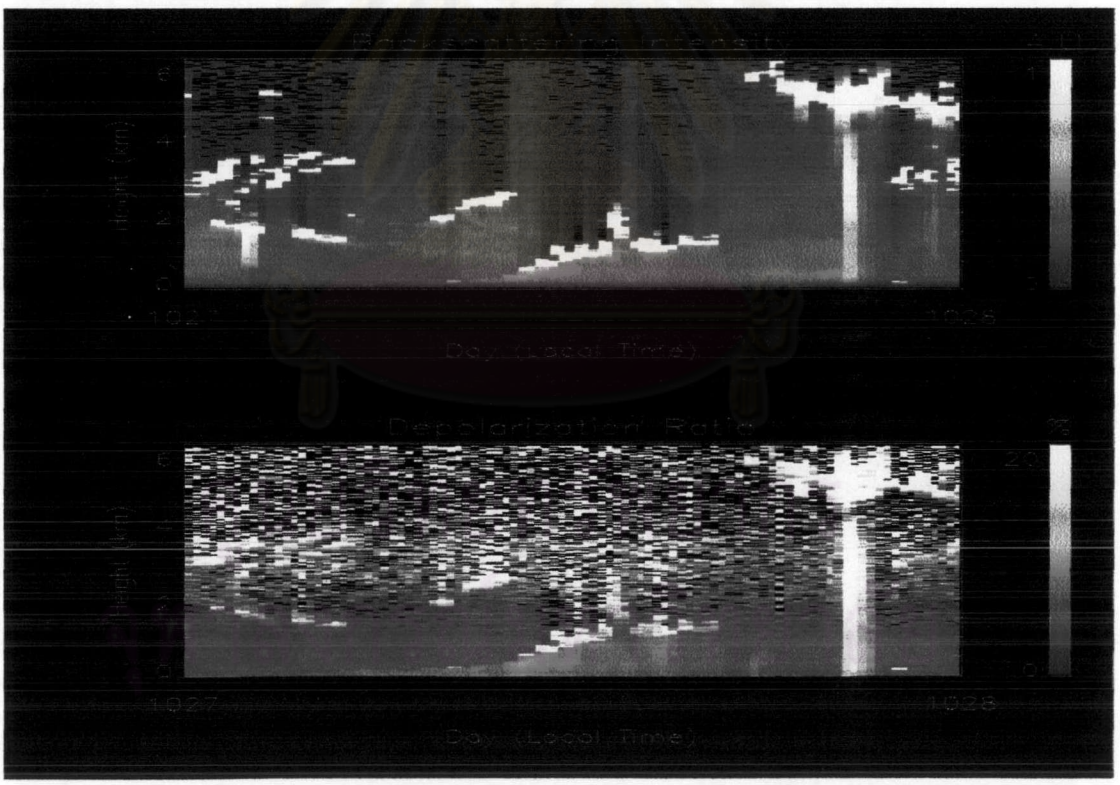

Figure 4.50 Backscattering intensity (up) and Depolarization ratio data that observed at 27th October 2001.

In this period, Fernald's method can not use to evaluate aerosol extinction coefficient because lower cloud induce multi scattering.

## 4.5 Discussion

According to backscattering intensity data, type of ABL could be divided into 3 periods i.e. A, B and C.

Period A, the ABL top height is almost constant at about 2 km through out this period because of subsidence from ridge of high pressure that covered the Observatory area. ABL variation occurs normally 2 times in a day, that is, ABL diurnal and nocturnal modification. ABL diurnal variation is formed by the influence of solar radiation in day time. This variation occurs at a few hundred meters in the morning to 2 km in the afternoon and it decays after sunset. ABL nocturnal variation is formed in night time by the influence of mechanical convection. According to lidar and radiosonde data, ABL variation may express as below;

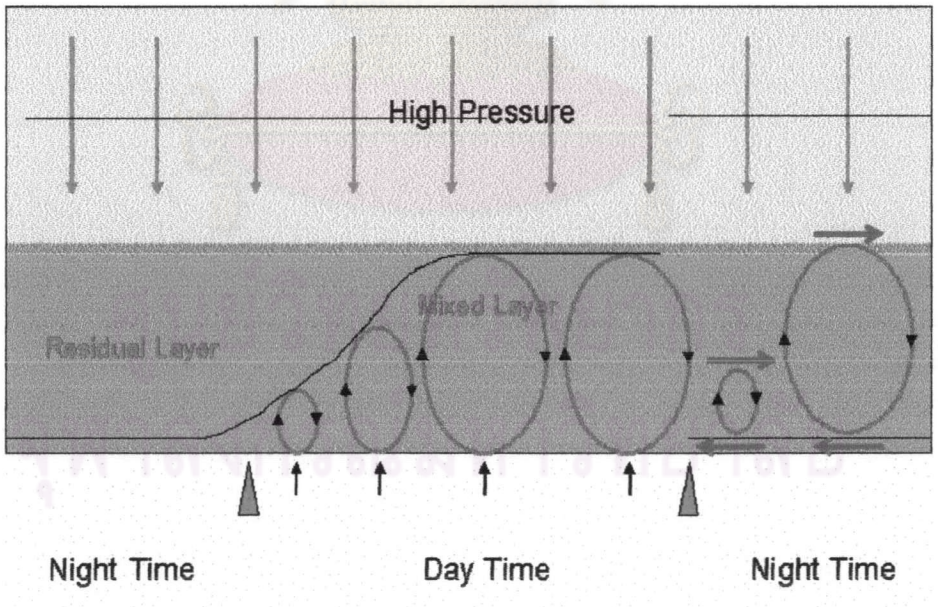


Figure 4.51 Schematic express ABL structure of Period A

2. Period B, the ABL top height increases from 2.5 km in February to 5 km in May. ABL modification also starts at about a few hundred meters in the morning and rose up to about 2 km or more in the afternoon by the influence of solar radiation (Figure 4.52). The ABL top height increases from early to late of this period by the influence of low pressure. Depolarization ratio data shows duration of low spherical aerosol that covered the Observatory increases, especially, at the transition time between Period B and C. ABL is covered by this kind of aerosol almost all the day.

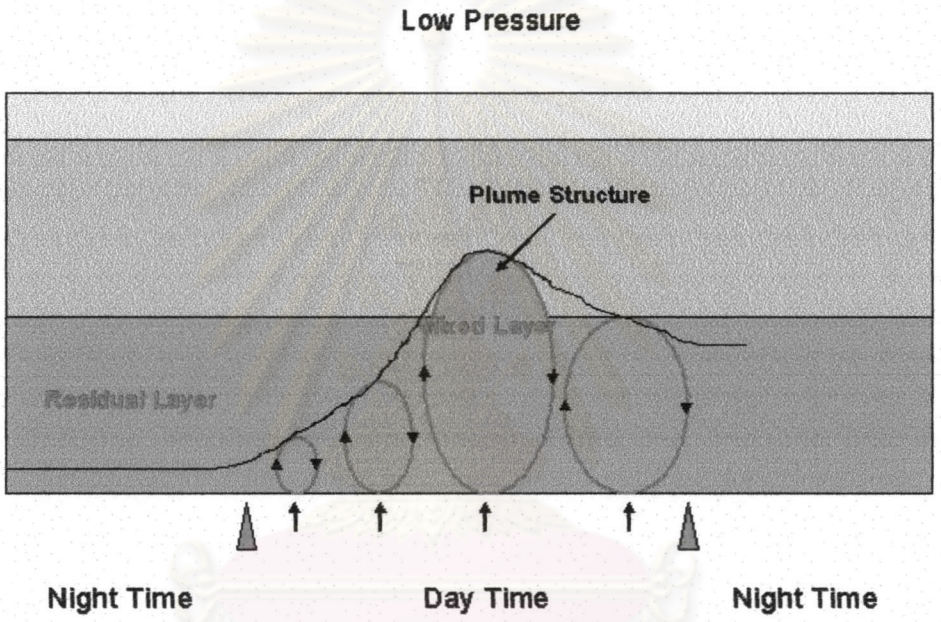


Figure 4.52 Schematic express ABL structure of Period B

3. Period C, the cloud covers the Observatory area almost all the day. The ABL modification follows the cloud base. During the time that cloud disappears, convective plumes were found in backscattering intensity data. Occasionally, cloud base height continuously increases from a few hundred meters in the morning to 5 – 6 km at midnight (Figure 4.53).

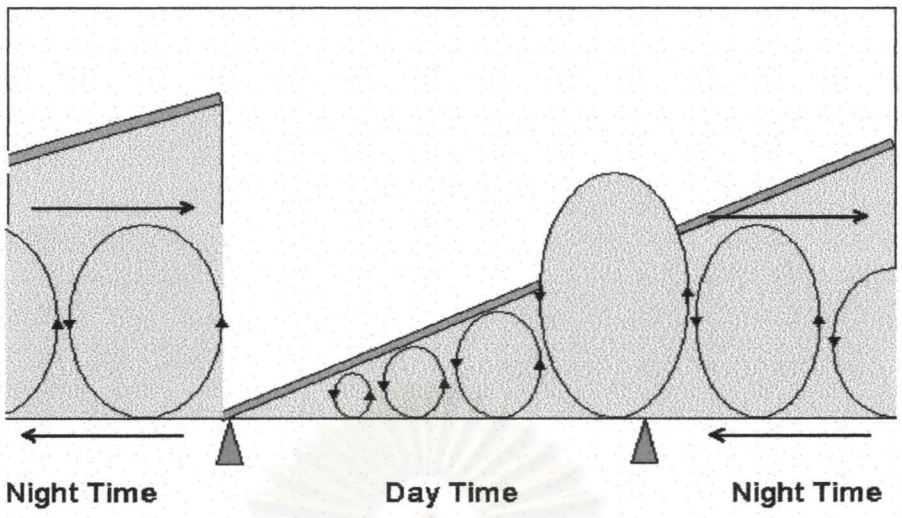


Figure 4.53 Schematic express ABL structure of Period C

The backscattering intensity data shows very low aerosol content and it becomes almost zero in the later part of this period. According to Takeuchi (2000), the amount of fine particle is much larger than that of coarse particle at Sri Samrong. Especially in rainy season the fine particle reduces down to one fifth (Figure 4.54). The depolarization ratio data shows, the Observatory area is covered by low spherical aerosol. The fact that the cloud base height increases continuously may came from the influence of condensation of water vapor prevents adiabatic process. In this period, vertical distribution profile of relative humidity is very high at about 80% – 90% from surface to 7 km. Vertical distribution profile of potential temperature gradient is almost constant.

In conclusion, ABL can divide into three periods by backscattering intensity data, namely, Period A, B and C. Top of ABL is about 2 km and almost constant all the day in Period A. For Period C, ABL top height is varies through this period. In this study, data that collected in February 1999 and March 2002 had been select to analyze. Top of ABL is about 3 km in February 1999 and about 5 km n March 2002. For Period C, ABL varies under cloud base that increase continuously through a day, from a few hundred meter to 5 – 6 kilometer in the next day morning.

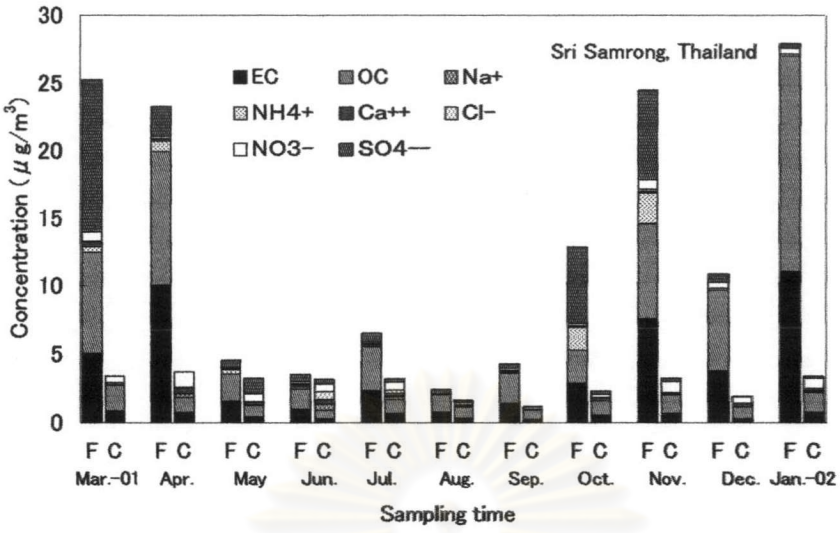


Figure 4.54 Concentration of chemical species in Sri Samrong. (Takeuchi; 2000)

However, this study is not so clear for ABL study because continuously lidar data is need to investigate ABL variation. In addition, more radiosonde data is also need for compare with lidar data.